Arabian Journal of Chemistry (2023) **16**, 104812

King Saud University

Arabian Journal of Chemistry

www.ksu.edu.sa
www.sciencedirect.com

ORIGINAL ARTICLE

Sulfated modification, basic characterization, antioxidant and anticoagulant potentials of polysaccharide from *Sagittaria trifolia*

Yang Zhang [a,1], Yihui Liu [a,1], Gaoyang Ni [a], Jiahao Xu [a], Yuping Tian [a], Xingyu Liu [a], Jia Gao [b], Qi Gao [a], Yingchao Shen [b,*], Zhaowei Yan [c,*]

[a] *School of Biology and Food Engineering, Changshu Institute of Technology, Changshu 215500, Jiangsu, China*
[b] *Department of Orthopedics and Traumatology, Changshu Hospital Affiliated to Nanjing University of Chinese Medicine, Changshu 215500, Jiangsu, China*
[c] *Department of Pharmacy, The First Affiliated Hospital of Soochow University, Suzhou 215006, Jiangsu, China*

Received 23 December 2022; accepted 11 March 2023
Available online 18 March 2023

KEYWORDS

Polysaccharide;
Sagittaria trifolia;
Sulfated modification;
Antioxidation;
Anticoagulation;
Degree of substitution

Abstract To discover novel antioxidants and anticoagulants for the prevention and treatment of cardiovascular diseases remains ongoing concern. *Sagittaria trifolia* is a commonly consumed aquatic vegetable with highly nutritious value and wide planting area in China. Polysaccharides are the major bioactive constituents, but little information is available on anticoagulant potential. In this work, a polysaccharide from *S. trifolia* (PST) was modified by sulfation to produce four sulfated derivatives (SPST-1 ~ 4), and their antioxidant and anticoagulant potentials were evaluated. Various means of analysis confirmed the success of sulfation on PST. The unmodified PST possessed notable antioxidant and pro-coagulant activities. To some extent, sulfated modification reduced the antioxidant capacity of PST with the increase of degree of substitution (DS), but for the derivative SPST-4 with moderate DS and smallest molecular weight (MW) exerted better antioxidant activity, in particular of scavenging nitrogen-containing radicals. Interestingly, sulfation reversed the innate activity of PST from pro-coagulation to anticoagulation, which highly depended on DS. The derivative SPST-3 with highest DS and moderate MW elicited promising anticoagulant potential, particularly at concentration of 5.00 mg/mL, which was superior to that of heparin (pos-

* Corresponding authors.
E-mail addresses: csfy045@njucm.edu.cn (Y. Shen), yanzwsuzhou@163.com (Z. Yan).
[1] These authors contributed equally.

Peer review under responsibility of King Saud University.

Production and hosting by Elsevier

https://doi.org/10.1016/j.arabjc.2023.104812

itive control) in the aspect of prolonging thrombin time and prothrombin time. Herein, the present contribution would give evidence that PST and sulfated derivatives SPST-3 and SPST-4 own potentials to be developed as hemostatic, anticoagulant, and antioxidant candidates, respectively.

1. Introduction

Aging-associated diseases bring great threat to the health of the elderly, among them, cardiovascular diseases (CVDs) are still the leading cause of death and one of the most common reasons that result in disabilities worldwide (Chen et al., 2021, Cheong et al., 2022). CVDs comprise a series of diseases that harm blood vessels or heart, such as heart failure, arrhythmia, stroke, coronary artery disease, peripheral artery disease, and other complications relating to vascular or cardiac problems (Mensah et al., 2019). Owing to the fact that CVDs become much more prevalent with age, thus, with the aging of the population, the incidence of CVDs is expected to increase dramatically (Evans et al., 2020). Actually, CVDs have led to over 17 million deaths all over the world, if this trend continues, the number of deaths caused by CVDs would surpass 23 million by 2030 (Amini et al., 2021). Indeed, it has been predicted that by 2035 nearly one in four individuals will be 65 years or older. Thrombotic disorder is responsible for the majority of cardiovascular events (Accurso et al., 2020). Under physiological conditions, hemostasis ensures the normal flow of blood in circulation and prevents life-threatening blood loss. Various coagulation factors, such as fibrinogen, thrombinogen and thrombin play important roles in hemostasis balance (Khalid et al., 2018). However, under abnormal or pathological conditions, disturbed hemostasis accelerates the formation of thrombi, which triggers or deteriorates CVDs. Thus, the timely and regular anticoagulant therapy is essential to the precaution and treatment of CVDs when facing thrombotic disorders (Zhang et al., 2020). In addition to thrombosis, the increased level of free radicals induced by oxidative stress equally plays a vital role in deteriorating CVDs. Numerous investigations have verified that overproduced free radicals are linked to the development of inflammation, apoptosis, hypertension, and atherosclerotic plaque (Panda et al., 2022). Antioxidants possess abilities to lower the increased free radicals, thereby potentiating the effects of anticoagulants, which would notably benefit the patents with CVDs.

Despite that unfractionated heparin and low-molecular-weight heparins are the clinical first-line drugs prescribed to cure thrombotic disorders, the bleeding risk associated with the use of these anticoagulant agents limits their clinical applications, particularly for cancer patients (Helfer et al., 2020). By contrast, the food-derived nutrients and phytochemicals have higher safety properties and are usually allowed to be consumed over a long period (Vilas-Boas et al., 2021). Many of them exert anticoagulant and antioxidant effects in humans, and could be extremely beneficial to the individuals who are suffering from CVDs or who have been diagnosed with CVDs (Stanger et al., 2012).

Polysaccharides refer to a class of macromolecules that consist of various monosaccharides linked by glycosidic bonds (Vo and Kim 2014). Currently, natural polysaccharides have attracted a great deal of interest due to diverse bioactivities, such as immuno-enhancement, antiviral, hypoglycemic, antioxidant, and anti-cancer properties (Ji et al., 2017). Some polysaccharides derived from foods, including jujube, green tea, pumpkin, and sea cucumber have been confirmed to be promising anticoagulant agents (Cai et al., 2013, Na et al., 2015, Liang et al., 2018, Zheng et al., 2019). These anticoagulant polysaccharides share certain similar characteristics in chemical constituents and structural parameters, of which sulfate group is one of the most common and important features of polysaccharides with anticoagulant potential (Kang et al., 2022). As highly acidic macromolecules, the sulfated polysaccharides are easier to interact with the positively charged groups in antithrombin to strengthen its anticoagulant function. Owing to non-specificity, the intensity of this interaction is usually proportional to the sulfate content (Mulloy 2005, Ciancia et al., 2010, Arata et al., 2017). In addition to naturally occurring sulfated polysaccharides, chemical modification provides a feasible way to introduce sulfate group into the polysaccharides that do not have innate sulfate (Chaouch et al., 2018). After sulfation, the inherent bioactivities of modified polysaccharides are usually improved, in particular of anticoagulant and antioxidant properties (Lu et al., 2012, Cai et al., 2018a, 2018b, Liang et al., 2018, Liu et al., 2018, Huang et al., 2019a, 2019b).

Due to peculiar flavors and abundant nutrients, the aquatic vegetables have gained increasing attention in the past few decades (Wang et al., 2015a, 2015b). China is home to about 300 aquatic plants, of which more than ten species are traditionally eaten as vegetables (Wang et al., 2018a). *Sagittaria trifolia* belonging to the Alismataceae family, is one of the most commonly consumed aquatic vegetables in China. It mainly grows in the shallow fresh-water marsh with annual planting area of about 20,000 ha. The edible tuber part of *S. trifolia* is a low-calorie and highly nutritive food, containing rich carbohydrates, dietary fibers, proteins, vitamins and essential minerals. The index of nutritional quality (INQ) of *S. trifolia* tuber is 2.1, much higher than those of other aquatic vegetables, such as lotus root (INQ = 1.54), water bamboo shoot (INQ = 1.53), and Chinese water chestnut (INQ = 1.04). The *S. trifolia* tuber can be eaten as a cooked dish or different processed food products, including crisp, biscuit, instant powder, and beverage (Zhang et al., 2021a, 2021b). The medicinal use of *S. trifolia* tuber was first recorded in the ancient medical book of *Mingyi Bielu* (2nd century BCE). Traditional Chinese medicine holds the opinion that *S. trifolia* tuber is non-toxic, cools blood to stop bleeding, relieves cough and stranguria, harmonizes the stomach, and nourishes the intestine (Pan and Liu 2006, Tan and Wang 2016). Recent studies have revealed that non-starch polysaccharides contribute most to the health-promoting benefits of *S. trifolia* tuber, such as antioxidant, hepatoprotective and immunostimulatory activities (Ke et al., 2018, Wang et al., 2018b, Zhang et al., 2019a, Zhang et al., 2019b, Deng et al., 2020, Gu et al., 2020a, Gu et al., 2020b, Gu et al., 2020c, Gu et al., 2020d). However, there is little information on the anticoagulant potential of *S. trifolia* polysaccharides. Previously, Gu *et al.* precipitated four polysaccharide fractions from *S. trifolia* tuber using ethanol of different strengths, and found that these fractions elicit promising antioxidant activities, and are naturally occurring sulfated polysaccharides with sulfate content ranging from 0.72% to 5.25% (Gu et al., 2020a, 2020b, 2020c, 2020d), which indicated that *S. trifolia* polysaccharides hold an important structural feature (sulfate group) of the anticoagulant polysaccharides, raising the question of whether *S. trifolia* polysaccharides possess anticoagulant capacity.

In the present investigation, we discussed the anticoagulant potential of *S. trifolia* polysaccharides for the first time. Based on the well-accepted view that the anticoagulant potential of polysaccharides is usually proportional to their sulfate contents, a series of sulfated derivatives were prepared via sulfation reaction to further enrich the sulfate density in *S. trifolia* polysaccharides. After basic characterization, these sulfated derivatives were evaluated to explore the probability of enhancing antioxidant and anticoagulant capacities of *S. trifolia* polysaccharides via sulfated modification, and to screen out the candidate that has great potentiality to be exploited.

2. Materials and methods

2.1. Materials

Fresh *S. trifolia* tubers were collected from a *S. trifolia* planting base on 08 November 2021, Suzhou, Jiangsu, China, and authenticated by Prof. Zhaowei Yan, Department of Pharmacy, The First Affiliated Hospital of Soochow University, Suzhou, Jiangsu, China. Voucher specimen with a code of No. STT2108 was preserved at School of Biology and Food Engineering, Changshu Institute of Technology, Changshu, Jiangsu, China. The fresh *S. trifolia* tubers were washed and cut into small pieces. After being dried at 60 – 70℃, these tuber pieces were grinded into powers and sieved to 60 mesh.

Diethylaminoethyl (DEAE)-52 cellulose, Sephadex G-200, vitamin C (VC), and 1, 1-diphenyl-2-picrylhydrazyl (DPPH) were obtained from Shanghai Macklin Biochemical Co., Ltd. (Shanghai, China). Standard monosaccharides, including glucose, galactose, fructose, xylose, rhamnose, mannose, arabinose, aminoglucose, ribose, glucuronic acid and galacturonic acid were purchased from Shanghai Yuanye Bio-Technology Co., Ltd. (Shanghai, China). T-series dextran standards were from Shanghai HuiCh Biotech Co., Ltd. (Shanghai, China).

Standard human plasma used for the evaluation of anticoagulant activity was provided by Siemens Healthcare Diagnostics Products GmbH (Marburg, Germany). Testing kits used for the determination of thrombin time (TT), prothrombin time (PT), activated partial thromboplastin time (APTT), and fibrinogen (FIB) were purchased from Nanjing Jiancheng Bioengineering Institute (Nanjing, Jiangsu, China). Yunnan Baiyao (negative control), a famous traditional Chinese hemostatic drug, was provided by Yunnan Baiyao Group Co., Ltd. (Kunming, Yunnan, China), and heparin (positive control) was from Shanghai Macklin Biochemical Co., Ltd. (Shanghai, China).

Other reagents, such as sulfamic acid (SA), 1-phenyl-3-methyl-5-pyrazolone (PMP), trifluoroacetic acid (TFA), sulfamic acid, and solvents were provided by Sinopharm Chemical Reagent Co. Ltd. (Beijing, China).

2.2. Polysaccharides extraction and preliminary purification

Ten grams of degreased *S. trifolia* tuber powders were soaked in distilled water at a liquid-to-solid ratio of 40: 1 for 12 h, and then extracted at 90℃ for 1.5 h. After cooling, the resulting mixture was filtered to obtain the filtrate, followed by being condensed under reduced pressure. The concentrated filtrate was precipitated with 4-fold volumes of anhydrous ethanol at 4℃ for 24 h. After removing most of ethanol, the remaining mixture was centrifuged at 1601 × g for 10 min to obtain the crude polysaccharides, which were sequentially subjected to Sevag deproteinization for three times. The deproteinated polysaccharides were dialyzed in a dialysis bag (retained molecular weight > 7000 Da) to remove small-molecular-weight compounds, and then lyophilized to give purified polysaccharides with yield of 5.12 ± 0.64% (Hu et al., 2019).

2.3. Polysaccharides isolation and further purification

One gram of purified polysaccharides was dissolved in 20 mL of distilled water, and then loaded on a DEAE-52 ion-exchange column chromatography, followed by stepwise elution with distilled water and NaCl solutions of different ionic strengths (0.1 – 0.5 M). The obtained eluents were respectively collected in test tubes (5 mL per tube), and the absorbance of eluent in each tube was determined to map elution curve (Fig. S1A). Based on the guidance of elution curve, the fraction with dominant amount (named as Fraction 1) was gathered, dialyzed, and lyophilized (Zhang et al., 2021a, 2021b).

Fraction 1 (F-1) was further purified by Sephadex G-200 filtration column chromatography (Li et al., 2020). Fifty milligrams of F-1 were dissolved in 5 mL of distilled water and carefully loaded on the gel column, and then eluted with deionized water at a flow rate of 0.5 mL/min. The eluent was collected (3 mL per tube), concentrated, and lyophilized to give homogeneous polysaccharide, which was renamed as PST (polysaccharide from *S. trifolia*) (Fig. S1B).

2.4. Sulfated modification on PST

The sulfamic acid (SA) method was conducted to modify PST, and four different sulfated derivatives were prepared via changing the mass ratios of PST to SA (Guo et al., 2010, Qian et al., 2015, Wang et al., 2020a, 2020b). In brief, certain amount of PST was added to a three-necked flask equipped with heating and stirring devices. After being dissolved in DMF, according to the mass ratios of PST to SA (1: 1, 1: 2, 1: 4, and 1: 8), different amounts of SA were added, respectively. The reaction was performed under vigorously stirring at 80 °C for 3 h. When the reaction was finished, the mixture was neutralized and precipitated with 4-fold volumes of anhydrous ethanol at 4℃ for 24 h. Then, the resulting precipitants were gathered, centrifuged, dialyzed, and lyophilized to produce the sulfated PSTs with different degrees of substitution, respectively. Accordingly, these sulfated derivatives were successively named as SPST-1 (1: 1), SPST-2 (1: 2), SPST-3 (1: 4), and SPST-4 (1: 8). The sulfate contents of PST and sulfated derivatives were determined by the barium chloride-gelatin turbidimetric method using a standard curve ($Y = 2.93X - 0.0017$, $R^2 = 0.9999$) calibrated with potassium sulfate (Song et al., 2019). The degree of substitution (DS) was reckoned based on the following formula:

$$DS = 1.62 \times S\%/(32 - 1.02 \times S\%) \quad (1)$$

Where S% refers to the sulfate content.

2.5. Determination of general physicochemical properties

2.5.1. Quantification of carbohydrates

Total carbohydrates content was determined by the phenol–sulfuric acid method using a standard curve ($Y = 11.68X + 0.0471$, $R^2 = 0.9977$) calibrated with glucose (Dubois et al., 1956).

2.5.2. Monosaccharide composition

Two milligrams of each sample were mixed with 2 mL of 2 M TFA in a hydrothermal reactor, which was placed in an oven at 110 °C for 5 h. After complete hydrolysis, the reaction mixture was co-evaporated with methanol to remove residual TFA. Then, the mixture was dissolved in distilled water, and reacted with 200 μL of 0.5 M PMP methanol solution and

200 μL of 0.3 M NaOH solution at 70℃ for 1.5 h. The reaction was quenched and neutralized with 0.3 M HCl, followed by being extracted with chloroform to obtain the PMP-labeled samples, which were filtered through 0.45 μm-pore Millipore filter for subsequent analysis. An UltiMate 3000 high-performance liquid chromatograph equipped with a Supersil ODS2 column (4.6 × 250 mm^2, 5 μm) and an UltiMate 3000 diode array detector (Thermo, Waltham, MA, USA) served as analyzer. The chromatographic conditions were: injection volume of 20 μL; mobile phase consisting of 0.05 M PBS (pH 6.8) and acetonitrile (82: 18, v/v); column temperature of 30 °C; detection wavelength of 245 nm; flow rate of 0.8 mL/min; run rate of 60 min. Commercially obtained monosaccharides served as standards (Hu et al., 2019).

2.5.3. Molecular weight

The molecular weight of each sample was determined by high-performance size- exclusion chromatography (HPSEC) (Li et al., 2020). In short, 2 mg of sample was thoroughly dissolved in 2 mL of ultrapure water, 20 μL of which was filtered through 0.45 μm-pore Millipore filter, and then injected into a TSK-gel G4000 PWXL column (7.8 mm × 300). A 1220 Infinity Ⅱ high-performance liquid chromatograph equipped with a refractive index detector (RID) (Agilent, Santa Clara, CA, USA) was conducted for the analysis. The chromatographic conditions were: mobile phase of ultrapure water; column temperature of 50 °C; RID temperature of 30 °C; flow rate of 1.0 mL/min; run rate of 30 min. A N2000 gel permeation chromatograph work station was used for recording and processing data. T-Series dextran standards were adopted to establish calibration curve for reckoning molecular weight.

2.5.4. Zeta potential

The zeta potential of each sample was determined by a Zetasizer Nano ZS900 nanoparticle size and potential analyzer (Malvern Instruments Co., Ltd., Malvern, United Kingdom). The tested sample was dissolved in deionized water to a concentration of 1.0 mg/mL, and measured at room temperature (Wei et al., 2020).

2.5.5. Fourier transform-infrared (FT-IR) spectroscopy

One milligram of each sample was ground with dried KBr powders and pressed into pellet. The characteristic functional groups in each sample were analyzed by a 650 FT-IR spectrophotometer (Gangdong Sci. & Tech. Co., Ltd., Tianjin, China) within 400 – 4000 cm^{-1} (Jia et al., 2021).

2.5.6. X-ray photoelectron spectroscopy (XPS)

The XPS analysis was conducted by a Physical Electronics PHI 5600 X-ray photoelectron spectrometer (Perkin-Elmer Corporation, Eden Prairie, MN, USA) using Al-Ka source for excitation. The chamber pressure was set below 2.7 × 10^{-7} Pa. The voltage and power were adjusted to 15 kV and 200 W, respectively. The spectra were recorded at a take-off angle of 45° under the energy of 23.5 eV with an energy step size of 0.1 eV. The obtained spectra were analyzed with a XPS PEAK 4.1 software (Wang et al., 2015a, 2015b, Zhai et al., 2021).

2.5.7. Scanning electron microscopy (SEM)

The test sample was scatteredly loaded on a silicon pellet, and then sputtered with a thin layer of gold powders under reduced pressure for the observation on a Regulus 8100 scanning electron microscope (Hitachi, Tokyo, Japan). The accelerating voltage was 5.0 kV, and image magnifications were set at 6000 × (Cai et al., 2018a, 2018b).

2.5.8. Atomic force microscopy (AFM)

The tested sample was dissolved in ultrapure water to a concentration of 1.0 mg/mL, and then filtered through 0.22 μm-pore Millipore filter. Ten microliters of filtrate were placed onto the freshly cleaved mica, and dried under reduced pressure. AFM observation was performed on a XE-120 atomic force microscope (Park Systems, Suwon, Korea) (Liu et al., 2021).

2.6. Antioxidant activity

2.6.1. Hydroxyl radical-scavenging activity

Two milliliters of PST or sulfated derivatives (0 – 2.5 mg/mL) were sequentially mixed with 1 mL of 0.75 mM 1, 10-phenanthroline solution (PBS, pH 7.4), 1 mL of 0.75 mM $FeSO_4$ solution, and 1 mL of 0.12% H_2O_2 solution, and the mixture was incubated at 37℃ for 60 min, and then the absorbance at 536 nm (A_s) was recorded. A mixture lacking PST or sulfated derivatives was used as the blank control (A_0), one lacking H_2O_2 served as the normal control (A_c), and VC replaced PST or sulfated derivatives to act as the positive control. The activity of PST or sulfated derivatives to scavenge hydroxyl radical was estimated by the following formula (Zhang et al., 2018):

$$\text{Hydroxylradical} - \text{scavengingrate}(\%) = (A_s - A_0) \times 100/(A_c - A_0) \quad (2)$$

2.6.2. DPPH radical-scavenging activity

Two milliliters of PST or sulfated derivatives (0 – 5.0 mg/mL) were mixed with 2 mL of 0.1 mM DPPH solution (being freshly dissolved in ethanol), and the mixture was reacted at room temperature for 30 min, and then the absorbance at 517 nm (A_s) was measured. The mixture lacking PST or sulfated derivatives was used as the blank control (A_0), one lacking DPPH served as the normal control (A_c), and VC replaced PST or sulfated derivatives to act as the positive control. The activity of PST or sulfated derivatives to scavenge DPPH radical was reckoned by the following expression (Zhang et al., 2018):

$$\text{DPPHradical} - \text{scavengingrate}(\%) = (A_s - A_0) \times 100/A_0 \quad (3)$$

2.7. Anticoagulant activity

The anticoagulant activity of each sample was appraised by a series of plasma clotting assays, including TT (thrombin time), PT (prothrombin time), APTT (activated partial thromboplas-

tin time), and FIB (fibrinogen) content. Normal saline (0.9% NaCl solution), Yunnan Baiyao (a famous traditional Chinese hemostatic drug) and heparin (a clinical first-line anticoagulant drug) were used as the blank control (BC), negative control (NC), and positive control (PC), respectively (Zhai et al., 2021). According to the results of preliminary experiments, the concentrations of each sample were designed from 0.31 to 5.00 mg/mL, and the concentrations of NC and PC were set as 5.00 mg/mL. Measurements for anticoagulant indicators were referenced to the methods described in the commercial assay kit instructions. Brief details were as follows:

For TT determination, 100 μL of normal saline embodying standard human plasma and tested sample were hatched at 37 °C for 1 min, and then added 200 μL of pre-warmed TT reagent, followed by recording the clotting time using a MC-4000 coagulometer (TECO Medical Instruments, Neufahrn, Germany). In PT assay, 100 μL of PT reagent were incubated at 37℃ for 30 s, and then added 50 μL of normal saline containing standard human plasma and tested sample. After incubation at 37 °C for 3 min, the clotting time was detected. In APTT assay, 100 μL of normal saline comprising standard human plasma and tested sample were incubated at 37 °C for 1 min beforehand, and added 50 μL of pre-warmed APTT reagent and co-incubated at 37 °C for 3 min, followed by being added 50 μL of 25 mM $CaCl_2$ solution, and then the clotting time was immediately determined. For FIB quantification, 100 μL of normal saline containing standard human plasma and tested sample were mixed with 900 μL of 20 mmol/L imidazole solution, from which 200 μL of mixture were taken out and hatched at 37 °C for 3 min. After being added 100 μL of FIB reagent, the clotting time was instantly recorded. The FIB content was reckoned according to the following calibration curve (Zhang et al., 2020):

$$\mathrm{LogT} = -0.821\mathrm{LogC} + 3.3316, \mathrm{R}^2 = 0.9976 \quad (4)$$

Where *T*- clotting time (s) and *C*-FIB content (mg/dL).

2.8. Statistical analysis

Data were represented as means ± SD ($n = 3$), and statistical assessment was performed with a SPSS software v19.0 (SPSS Inc., Chicago, USA) using one-way analysis of variance (ANOVA), where $P < 0.05$ was considered statistically significant.

3. Results and discussion

3.1. General physicochemical properties

3.1.1. Major chemical profiles

The degree of substitution (DS) is usually a vital factor that influences the bioactivities of sulfated polysaccharides (Huang et al., 2019a, 2019b). For sulfate-modified polysaccharides, DS can be mainly controlled by the amount of sulfating reagent, thereby modulating the innate bioactivities (Roman et al., 2017, Shalaby et al., 2018). To explore the effects of sulfated modification on PST, four sulfated derivatives (SPST-1 ~ 4) were manufactured via varying the mass ratios of PST to sulfamic acid (SA, a commonly used sulfating reagent). The carbohydrates, sulfates, DS, MW, and monosaccharide composition were determined and summarized in Table 1. It can be observed that PST is a naturally occurring sulfated polysaccharide with sulfate content of 3.78 ± 0.11%. After sulfated modification, the sulfate contents of resulting derivatives (SPST-1 ~ 3) were significantly ($P < 0.01$) elevated from 5.46 ± 0.10% to 12.22 ± 0.50% with the amount of sulfating reagent increasing from 1: 1 to 1: 4, and the corresponding DS was markedly ($P < 0.01$) heightened from 0.33 ± 0.01 to 1.01 ± 0.07, suggesting that the sulfation on PST had achieved successfully, and the increase of sulfating reagent was beneficial for DS enhancement (Qian et al., 2015, Wang et al., 2018c). However, when sulfating reagent exceeded 1: 4 to reach 1: 8 (SPST-4), the sulfate content begun to fall, and DS dropped to 0.79 ± 0.02, notably lower ($P < 0.05$) than that of SPST-3. The results were in accordance with previous findings that excessively large amount of sulfating reagent may lead to uneven reactions (Wang et al., 2009, Bai and Qian 2015). Moreover, the contents of total carbohydrates in sulfated derivatives decreased with the increase of sulfating reagent, and all of them were significantly ($P < 0.01$) less than that in PST (Table 1), which was consistent with those of published cases for the sulfated modification on polysaccharides from *Sargassum pallidum* (Xiao et al., 2019), defatted rice bran (Wang et al., 2009), and pumpkin (Liang et al., 2018), etc.

Table 1 Major chemical profiles of PST and sulfated derivatives.

Sample	Sample: SR (m/m)	Carbohydrates (w, %)	Sulfates (w, %)	DS	ξ-Potential (mV)	MW (kDa)	Monosaccharide composition (Mole ratio)
PST	1: 0	90.04 ± 2.80 ^{a}	3.78 ± 0.11 ^{a}	0.22 ± 0.01 ^{a}	−5.98 ± 0.99 ^{a}	576.9	Man: Glu: Gal: Arab = 4.02: 20.1: 7.11: 1.00
SPST-1	1: 1	77.47 ± 3.28^{b}	5.46 ± 0.10 ^{a}	0.33 ± 0.01^{a}	−10.7 ± 2.15^{b}	416.5	Man: Glu: Gal: Arab = 2.57: 2.07: 1.08: 1.00
SPST-2	1: 2	69.57 ± 2.17^{c}	8.81 ± 1.36^{b}	0.63 ± 0.13^{b}	−12.9 ± 0.60 ^{bc}	303.5	Glu: Gal: Arab = 7.34: 2.48: 1.00
SPST-3	1: 4	46.71 ± 2.31 ^{d}	12.22 ± 0.50^{c}	1.01 ± 0.07^{c}	−17.3 ± 0.31^{de}	255.7	Glu: Gal: Arab = 15.6: 2.81: 1.00
SPST-4	1: 8	42.23 ± 0.27 ^{d}	10.43 ± 0.17^{b}	0.79 ± 0.02^{b}	−15.7 ± 1.71 ^{cd}	129.6	Glu: Gal = 3.97: 1.00

Different superscript letters refer to significant differences ($P < 0.05$, or $P < 0.01$) in the same row. Abbreviations: SR (sulfating reagent), DS (degree of substitution), MW (molecular weight), Man (mannose), Glu (glucose), Gal (galactose), and Arab (arabinose).

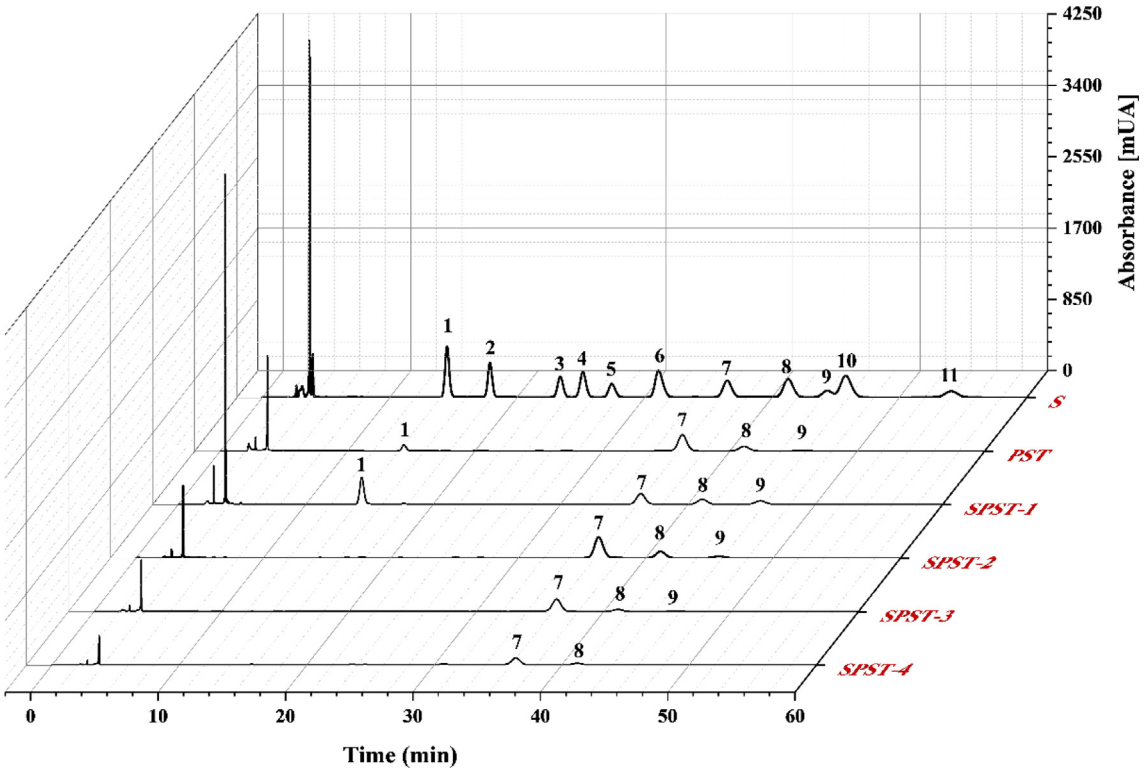

Fig. 1 The HPLC chromatograms of PMP-labelled PST and sulfated derivatives. S: standard monosaccharides. Peaks: (1) mannose, (2) glucosamine, (3) ribose, (4) rhamnose, (5) glucuronic acid, (6) galacturonic acid, (7) glucose, (8) galactose, (9) xylose, (10) arabinose, and (11) fructose.

Moreover, the stability of macromolecules in solution largely depends on the attractive and repulsive intermolecular forces. ξ-Potential is deemed as an effective indicator for characterizing the electrostatic interactions between particles (Wei et al., 2020). The ξ-potentials of PST and sulfated derivatives were depicted in Table 1. The ξ-potential of PST was − 5.98 ± 0.99 mV, and the negative charge could be contributed by the naturally occurring sulfates (Gutierrez et al., 2012, Caputo et al., 2019). After sulfation, ξ-potential of each sulfated derivative significantly ($P < 0.05$, or $P < 0.01$) decreased from − 10.66 ± 2.15 mV to − 17.33 ± 0.31 mV as compared with that of PST, which further confirmed that different sulfated modifications on PST have occurred. As anticipated, the downtrend in ξ-potential of sulfated derivatives generally corresponded to the increase of DS. The magnitude of ξ-potential is proportional to the charge density. Sulfated modification can enrich the charge density in PST, conferring sulfated derivatives more stable properties in solution, particularly for the counterparts with higher DS, due to the accumulation of intermolecular repulsive forces resulting from sulfates (Zhang et al., 2010, Cai et al., 2020).

From Table 1 and Fig. 1, it can also be noted that PST possesses a molecular weight (MW) of 576.9 kDa, and comprises mannose, glucose, galactose, and arabinose at molar ratios of 4.02: 20.1: 7.11: 1.00. After sulfated modification, with the increase of sulfating reagent, the MWs of each derivative were gradually reduced to the lowest level of 129.6 kDa, which decreased by 77.5% as compared with that of PST (Table 1). It has been reported that sulfation is usually accompanied by polysaccharide degradation, resulting in the reduction of MW (Liu et al., 2009, Xie et al., 2016, Kazachenko et al., 2021). Similarly, the monosaccharide compositions of sulfated derivatives underwent changes with the increase of sulfating reagent (Table 1 and Fig. 1). When sulfating reagent reached 1: 2 (SPST-2), the numbers of monosaccharides decreased to three kinds. With continuous elevation to 1: 8 (SPST-4), the numbers of monosaccharides were reduced to two kinds. The results implied that sulfation process might degrade the backbone and side chains of PST (Guo et al., 2010, Liang et al., 2018, Xiao et al., 2019, Wang et al., 2020a, 2020b). These results were also in accordance with the above-mentioned phenomenon that total carbohydrates content in sulfated derivatives declined after sulfation (Table 1), probably owing to the fact that the dropped small-molecular-weight saccharides could be cleared by dialysis operation, resulting in the gradual reduction of total carbohydrates and monosaccharides in sulfated derivatives of PST.

3.1.2. FT-IR analysis

Due to distinct vibrations, the FT-IR is extensively utilized to analyze the functional groups and characteristic absorption peaks of diverse biomacromolecules, particularly for polysaccharides (Gu et al., 2020a, 2020b, 2020c, 2020d). The FT-IR spectra of PST and sulfated derivatives were displayed in Fig. 2. The strong signal peaks between 3600 and 3200 cm^{-1} were attributed to the –OH stretching vibration (Cai et al., 2018a, 2018b), and the weak peaks between 3000 and 2700 cm^{-1} were due to the C—H stretching and bending vibra-

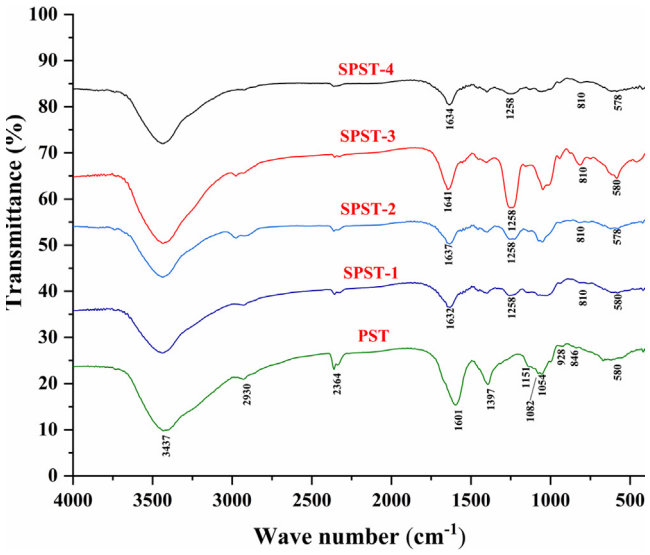

Fig. 2 The FT-IR spectra of PST and sulfated derivatives.

tions of —CH_2— and —CH_3 (Chen et al., 2019). Moreover, the peaks at around 1650 – 1600 cm^{-1} were assigned to the —C═O asymmetric stretching vibrations (Zeng et al., 2020). The peaks at 1397 cm^{-1} were associated with the C—O stretching vibration (Wang et al., 2019a, 2019b). The signals at 1151, 1082, and 1054 cm^{-1} could be assigned to the C—O—C stretching vibration of glucosidic bonds or the C—O—H bending vibration of side chains, demonstrating that PST comprises the pyranose moiety (Nie et al., 2018). What's more, any noticeable absorption peaks at 890, 925, and 1074 cm^{-1} were not found, but one of the typical absorption peaks for pyranose was obviously presented at around 580 cm^{-1} (Song et al., 2019, Zeng et al., 2020), which further confirmed that PST is composed of pyranose instead of furanose. In addition, the weak signal at 846 cm^{-1} could be assigned to the α-configuration of pyranosidic bonds (Chen et al., 2016, Zeng et al., 2020). It is well accepted that absorption peaks at about 810 and 1258 cm^{-1} are closely linked to the symmetric stretching vibration of C—O—S and the asymmetric —S═O stretching vibration in polysaccharide molecules (Liang et al., 2018). As compared with PST, it is apparent that the two peaks at 810 and 1258 cm^{-1} were emerged after sulfation, suggesting that sulfuric ester might be introduced at C-2 position of pyranose moiety (Hou et al., 2017). Furthermore, the peak intensity is likely to be in proportion to DS. The two peaks at 810 and 1258 cm^{-1} of sulfated derivatives tended to be stronger and deeper with the increase of DS, which was in line with the findings discovered by Zhang *et al* (Zhang et al., 2010).

3.1.3. XPS analysis

The XPS is widely used to analyze the surface elements of substances. Recently, XPS has begun to be applied for the characterization of polysaccharides (Wang et al., 2015a, 2015b, Zhai et al., 2021). The XPS spectra of PST and sulfated derivatives were exhibited in Fig. 3. The selected element signals were S2p, C1s, and O1s, which are more related to sulfated polysaccharides. As shown in Fig. 3A, the wide-survey XPS spectra confirmed the presence of S2p, C1s and O1s in PST and sulfated derivatives at the binding energies of 169.08 eV, 285.08 – 286.08 eV, and 532.08 eV, respectively. The signals at 169.78 eV were assigned to S2p (S^{6+}) (Wang et al., 2015a, 2015b). From Fig. 3B, it can be observed that signals at 169.78 eV were remarkedly enhanced from 2495.24 to 28410.1 counts/s after sulfation, and the increasing trend was consistent with that of DS (Table 1). Fig. 3C represented the C1s spectra of PST and sulfated derivatives. There are five different types of C atoms in PST: the peak at 295.38 eV could be due to the transition from 1s to the σ^* state (Yamamoto et al., 2001), the peak at 292.38 eV could be attributed to pure carbon (Uda et al., 2021), and the peak at 287.68 eV could be assigned to the photoemission of —C═O. While the two peaks at 286.18 and 284.68 eV could be responsible for the functionalized carbon (C—O, C—N, or C—S) and non-functionalized carbon (C—C and C—H), respectively (Zhai et al., 2021). Sulfation greatly changed the types of C atoms. As for sulfated derivatives (SPST-1 ∼ 4), the peaks at 295.38 and 292.38 eV disappeared and peak at 287.68 eV weakened, while the peaks at 286.18 and 284.68 eV were enhanced, which further confirmed the evidence of sulfation (Wang et al., 2015a, 2015b). As shown in Fig. 3D, the shift and enhancement of O1s signals after sulfation can be noted. The high binding energy of 532.08 eV could be owing to the electron-withdrawing groups of sulfated derivatives, and different shapes of O1s peaks were more likely to be related to a much larger component of —S═O (Essayem et al., 2007, Wang et al., 2015a, 2015b). These changes accorded with the observation of FT-IR analysis, where the two peaks at 810 and 1258 cm^{-1}, representing C—O—S and —S═O, were enhanced after sulfation (Fig. 2).

3.1.4. Morphological analysis

The stereo-morphologies of polysaccharides are hard to be exhibited visually, fortunately, the SEM provides a means to observe the fine structures of polysaccharide surface under magnification (Chen et al., 2020). As presented in Fig. 4A, PST appeared almost a smooth surface with partly lumpy uplift and pitted depression. After sulfation, several rod-shape and oval particles appeared on the surface of SPST-1, and some sheet-shape fragments were also observed (Fig. 4B). In comparison with SPST-1, the surface of SPST-2 was substantially transformed into fragmentation shapes (Fig. 4C). Furthermore, with increasing sulfating reagent, SPST-3 surface began to emerge crisscross grooves with honeycomb shape (Fig. 4D). However, with the continuous elevation of sulfating reagent, the interstitial spaces on the surface of SPST-4 became wider and deeper (Fig. 4E). These observations generally complied with the results described in Table 1 that degradation usually occurs when polysaccharide is subjected to sulfation, and degradation degree is in proportion to the amount of sulfating reagent. Structural degradation is inevitable to accompany the breakages of glycosidic bonds, which can be deteriorated by the increase of sulfating reagent, leading to the fragmentation or aggregation of polysaccharide molecules (Du et al., 2016, Wang et al., 2020a, 2020b).

The AFM is another useful tool to characterize morphologies of polysaccharides, especially for the acquirement of spatial distribution information (Chen et al., 2019, Chen et al., 2020). The 2D and 3D AFM images of PST and sulfated derivatives were exhibited in Fig. 5. As compared with PST (Fig. 5A), sulfated derivatives (SPST-1 ∼ 4) displayed more lumps and irregular agglomerations (Fig. 5B – 5E), suggesting

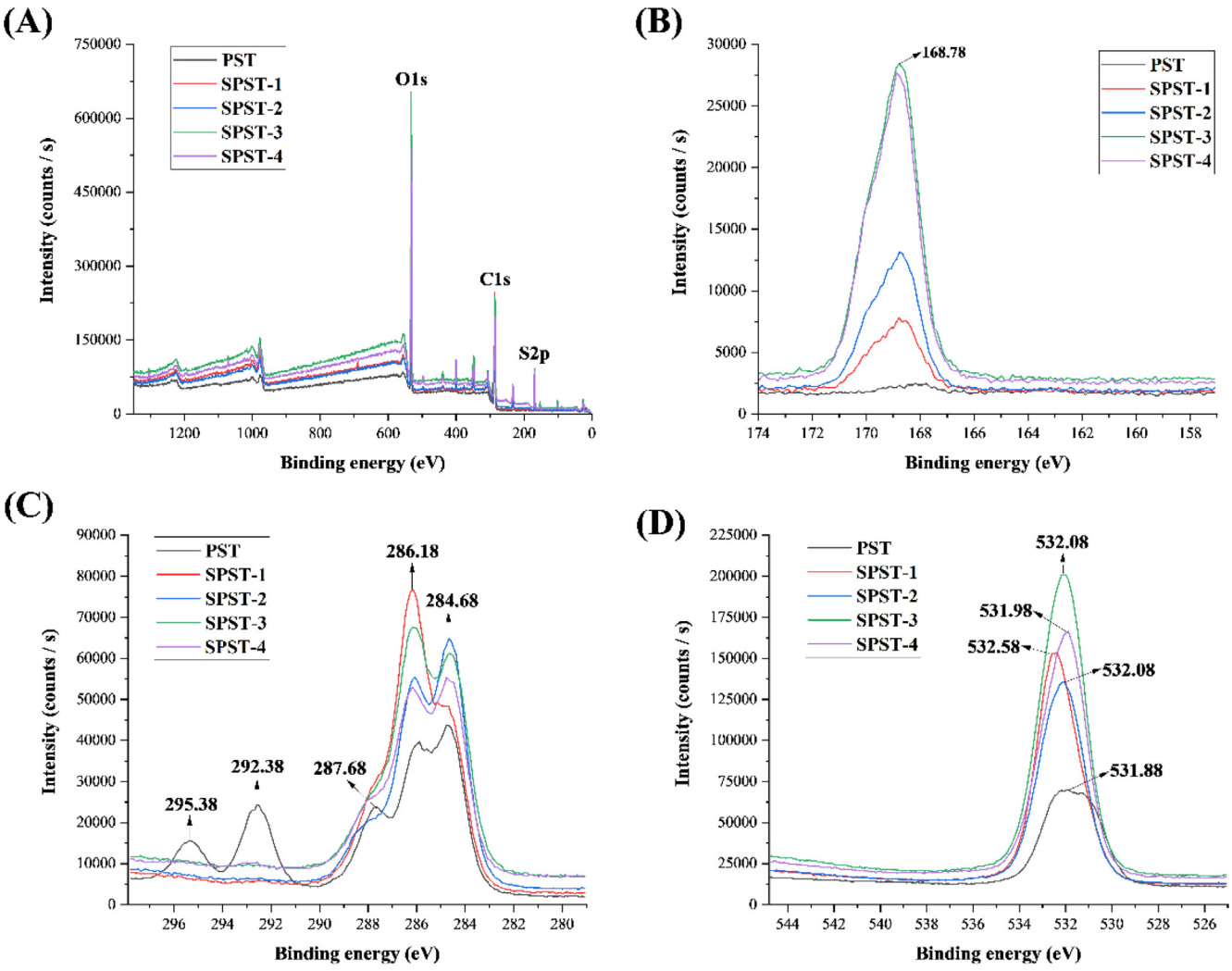

Fig. 3 The wide-survey XPS spectra (**A**), S2p spectra (**B**), C1s spectra (**C**), and O1s spectra (**D**) of PST and sulfated derivatives.

that these sulfated derivatives are more apt to gather together and possess more branched and entangled structures (Wang et al., 2017). The results could be probably attributed to the fact that more polar groups were freed due to the cleavage of glycosidic bonds after sulfation, and the newly released polar groups would potentiate the formation of additional hydrogen bonds, resulting in more intermolecular and intramolecular interactions with each other (Gao et al., 2017). Moreover, the net vertical heights of PST and sulfated derivatives were 76.2 (PST), 92.3 (SPST-1), 129.8 (SPST-2), 141.4 (SPST-3), and 100.0 nm (SPST-4), respectively, which were likely to be in line with the changes of DS (Table 1). Among them, SPST-3 had the highest DS of 1.01, and coincidently its height was also taller than other samples, which may be due to the reason that SPST-3 contains more sulfates rich in hydroxyl (H-donor and H-acceptor) and carbonyl (H-acceptor) groups, providing more opportunities to form hydrogen bonds (Gao et al., 2017). AFM observations were equally consistent with those of SEM outcomes that the surface of PST was transformed from almost smooth shape to fragmentation and hollowly honeycombed shapes after sulfation (Fig. 4).

3.2. Antioxidant activity

Hydroxyl radical is the most common oxygen-containing free radical, it has highly reactive property, and can react with almost any molecules in living cells (Hou et al., 2020). While, DPPH radical is a nitrogen-containing free radical with stable property, if a substance can efficiently quench DPPH radical, which would suggest that the tested substance possesses higher scavenging capacity against free radicals, especially for reactive nitrogen species (RNS) (Zheng et al., 2015). Hence, hydroxyl and DPPH radicals usually serve as models to estimate the antioxidant potential of tested sample.

Fig. 6 presented the scavenging abilities of PST and sulfated derivatives against hydroxyl and DPPH radicals. As shown in Fig. 6A, PST and sulfated derivatives exerted scavenging capacities against hydroxyl radical within the concentrations of 0 – 2.5 mg/mL. The activity increased with the increase of sample concentration, and the highest scavenging rates achieved at 2.5 mg/mL were from 77.32 ± 5.46 to 96.47 ± 4.03%. The half maximal inhibitory concentration (IC_{50}) value is a useful indicator to directly reflect the antioxidant capacity of tested sample. It is defined as the concentration of sample

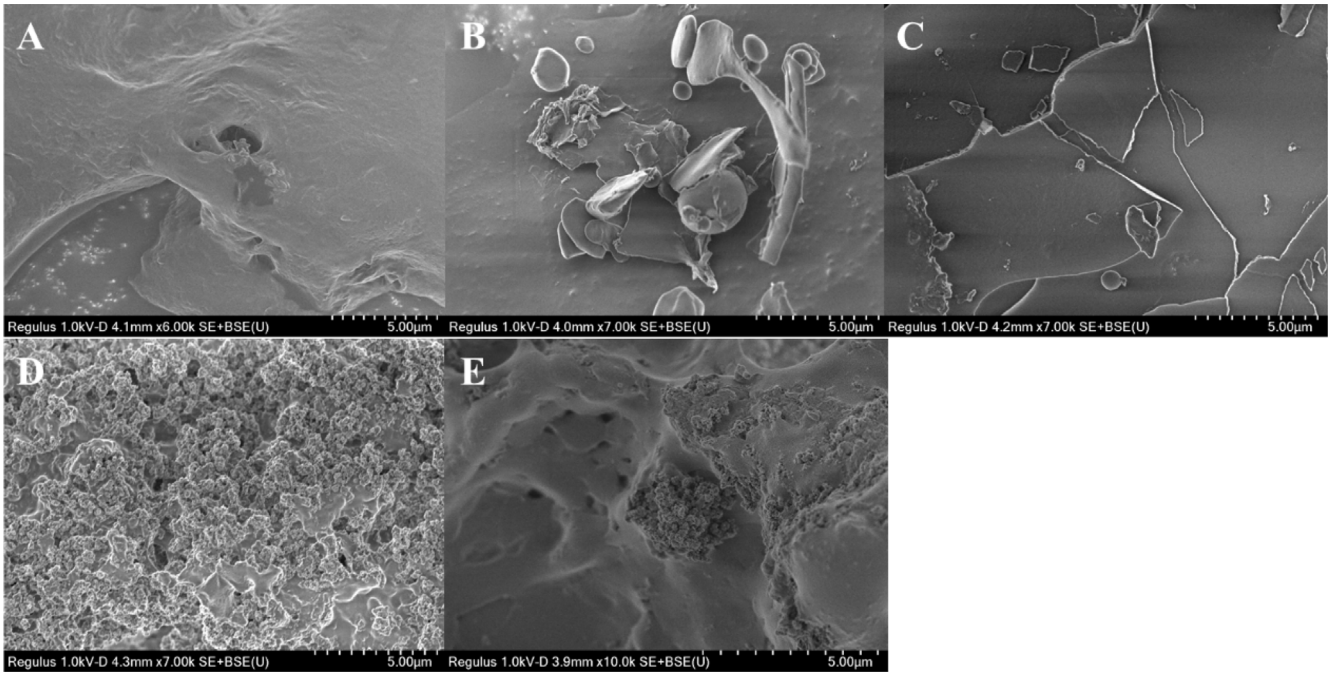

Fig. 4 The SEM images of PST (**A**), SPST-1 (**B**), SPST-2 (**C**), SPST-3 (**D**) and SPST-4 (**E**).

that is required to inhibit 50% of the initial concentration of free radicals. The smaller the IC_{50} value, the stronger the antioxidant capacity of tested sample (Xie et al., 2016). As shown in Fig. 6B, all the IC_{50} values of PST and sulfated derivatives were markedly ($P < 0.01$) higher than that of the positive control (VC). When compared with unmodified polysaccharide (PST), the IC_{50} values of sulfated derivatives SPST-1 and SPST-2 significantly ($P < 0.01$) increased. Unexpectedly, with the continuous increase of sulfating reagent, the IC_{50} values of SPST-3 and SPST-4 decreased, remarkably ($P < 0.05$ or $P < 0.01$) lower than those of SPST-1 and SPST-2, and even lower than that of PST (0.81 ± 0.05 mg/mL for SPST-4 *vs.* 0.91 ± 0.07 mg/mL for PST), but significant differences were not observed ($P > 0.05$). Similarly, as shown in Fig. 6C, within the concentrations spanning from 0 to 5.0 mg/mL, PST and sulfated derivatives elicited scavenging activities against DPPH radical. The DPPH radical-scavenging rate was elevated with the increase of concentration, and the highest levels at 5.0 mg/mL ranged from 77.21 ± 2.21 to 93.88 ± 4.11%. As shown in Fig. 6D, all the IC_{50} values of PST and sulfated derivatives were significantly ($P < 0.01$) higher than that of VC. As compared with PST, the IC_{50} values of SPST-1 ~ 3 were remarkably ($P < 0.01$) heightened, but that of SPST-4 noticeably ($P < 0.01$) decreased, suggesting that the DPPH radical-scavenging capacity of SPST-4 is stronger than PST.

These results suggested that sulfated modification could reduce the hydroxyl and DPPH radicals-scavenging capacities of PST to some extent, which were in accordance with the counterparts of polysaccharide from *Cyclocarya paliurus* (Xie et al., 2016). The free radicals-scavenging activity of polysaccharides mainly depends on their hydroxyl groups, which can donate hydrogen to quench free radicals (Chen et al., 2011). Generally, introduction of sulfate groups into polysaccharides can enhance antioxidant activity, due to the fact that O–H bond in sulfate group possesses weaker dissociation energy than that in hydroxyl group, resulting in stronger hydrogen-donating capacities to scavenge free radicals (Chang et al., 2010). However, in the present investigation, the antioxidant activity of SPST-3 with the highest DS (1.01) was weaker than that of SPST-4 with a relatively lower DS (0.79), suggesting that other physicochemical parameters equally influence the bioactivities of sulfated polysaccharides in addition to DS. Actually, the molecular weight (MW) of macromolecules is also one of the major factors that affect antioxidant activity (Hu et al., 2018), and the macromolecule with smaller MW is more inclined to interact with free radicals effectively (Zhang et al., 2018). The MW of SPST-4 (129.6 kDa) is smaller than that of SPST-3 (255.7 kDa), which would confer SPST-4 a stronger antioxidant activity, even though it has lower DS than SPST-3. Certainly, other structural physicochemical parameters, such as degree of branching, glycosidic linkage and conformation, are also the factors that influence the antioxidant activities of sulfated polysaccharides (Xie et al., 2016). The exact structure-antioxidation relationship of sulfated polysaccharides needs further studies. More importantly, for SPST-4, the promising antioxidant candidate needs to be verified using more antioxidant models, such as reducing power assay, ferrous chelating capacity, and β-carotene bleaching assay. These explorations should also be carried out in the future.

3.3. Anticoagulant activity

Blood coagulation and anticoagulation are normally in dynamic balance to retain the homeostasis of circulation system, but when the activity of hemostatic pathway outperforms the regulation of anticoagulant factors, thrombosis usually occurs, leading to the onset and aggravation of CVDs (Lippi et al., 2011). It is therefore important to supplement anticoag-

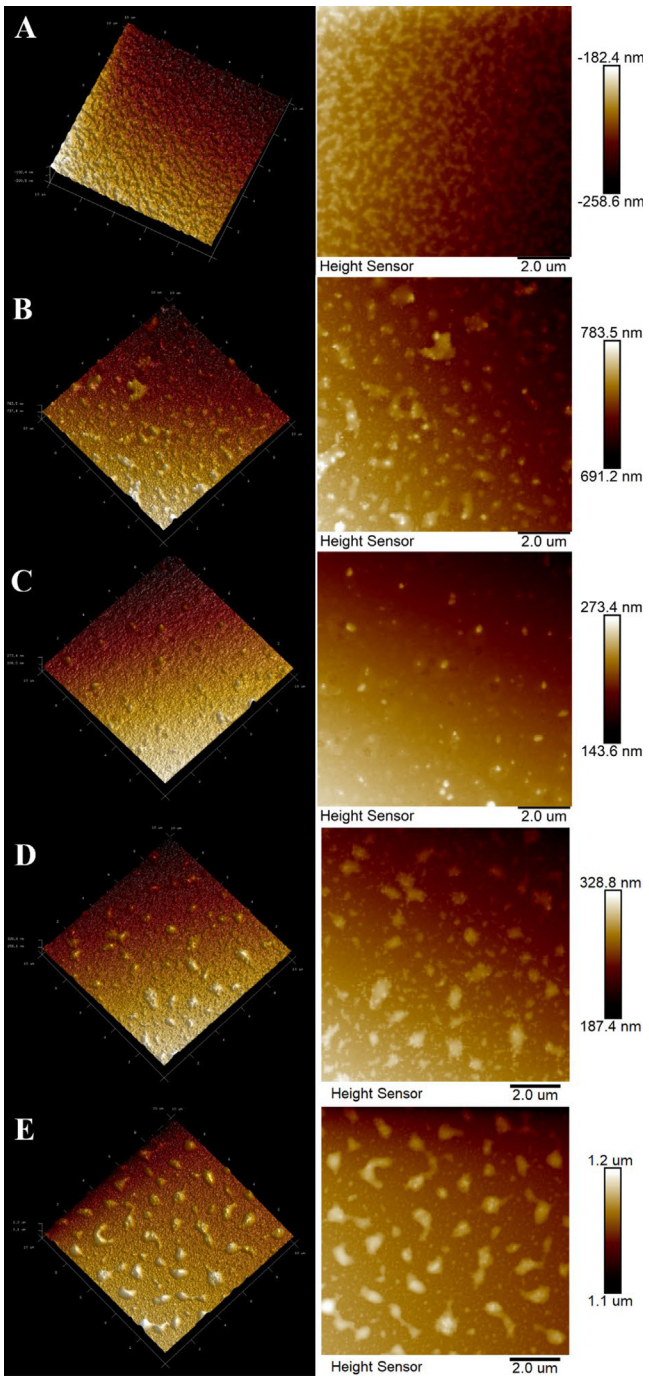

Fig. 5 The AFM images of PST (**A**), SPST-1 (**B**), SPST-2 (**C**), SPST-3 (**D**) and SPST-4 (**E**).

ulants regularly for the prevention and treatment of CVDs. In the present investigation, to assess the anticoagulant potential of PST and sulfated derivatives (SPST-1 ~ 4), several anticoagulant biomarkers, including thrombin time (TT), prothrombin time (PT), activated partial thromboplastin time (APTT), and fibrinogen (FIB) content were quantified to clarify the possible mechanisms on inhibition of blood clotting. Normal saline (0.9%NaCl solution) was used as blank control (BC), and heparin at a concentration of 5.00 mg/mL served as positive control (PC). Yunnan Baiyao (YNBY) is a well-known traditional Chinese medicine that has been prescribed as a hemostatic drug for over 100 years (Tang et al., 2009). Thus, YNBY at a concentration of 5.00 mg/mL acted as the negative control (NC).

The effects of PST and sulfated derivatives on TT were first appraised. As shown in Fig. 7A, the capabilities of PST on TT prolongation were significantly ($P < 0.01$) lower than that of BC at concentrations ranging from 0.31 to 2.50 mg/mL. When concentration was 5.00 mg/mL, TT value of PST reached 9.80 ± 0.56 s, still shorter than that of BC (12.53 ± 1.12 s), but significant difference was not observed ($P > 0.05$). After sulfation, TT values of sulfated derivatives were gradually elevated in a concentration-dependent manner ($P < 0.05$ or $P < 0.01$), of which the TT value of SPST-3 at a concentration of 1.25 mg/mL was 19.23 ± 0.23 s, notably ($P < 0.01$) longer than that of BC, and when concentration was heightened to 5.00 mg/mL, TT value of SPST-3 reached 36.20 ± 1.23 s, not only markedly ($P < 0.01$) higher than that of BC, but also significantly ($P < 0.01$) longer than that of PC (30.8 ± 2.52 s). But for SPST-4, the effect on increasing TT was inferior to SPST-3. As compared with NC, lower concentrations of PST exhibited certain effects on shortening TT, at a concentration of 0.31 mg/mL, the TT value was 3.97 ± 0.15 s, shorter than that of NC (5.17 ± 0.87 s). With the increase of concentration, TT values of PST were raised and reached 9.80 ± 0.56 s at a concentration of 5.00 mg/mL, significantly ($P < 0.01$) higher than that of NC, but shorter than that of BC. After sulfation, TT-shortening capacity of PST was moderately reversed to the TT-prolonging activity. For example, the TT value of SPST-3 at a concentration of 0.31 mg/mL was 10.60 ± 1.40 s, which had been dramatically ($P < 0.01$) longer than that of NC. The results indicated that unmodified PST possesses certain TT-shortening activity, while sulfated modification could convert the intrinsic effect into TT-prolonging capability via common coagulation pathway (Adrien et al., 2017).

The effects of PST and sulfated derivatives on PT were then evaluated. As shown in Fig. 7B, as compared with BC, the activities of PST on PT extension were considerably ($P < 0.01$) lower at concentrations spanning from 0.31 to 1.25 mg/mL. When concentration exceeded 2.50 mg/mL, PT values (11.40 ± 1.05 s at 2.50 mg/mL and 15.30 ± 1.14 s at 5.00 mg/mL) of PST were equivalent to that of BC (13.40 ± 0.46 s), but significant differences were not found ($P > 0.05$). After sulfation, PT values of sulfated derivatives were steadily raised in a concentration-dependent manner ($P < 0.05$ or $P < 0.01$). Among them, the PT values of SPST-2 at 5.00 mg/mL, SPST-3 at 2.50 and 5.00 mg/mL as well as SPST-4 at 5.00 mg/mL were markedly higher ($P < 0.01$) than that of BC, especially for SPST-3 at 5.00 mg/mL, the PT value of which reached 37.97 ± 1.21 s, even significantly ($P < 0.05$) higher than that of PC (32.63 ± 5.23 s). Being similar to the influence on TT, lower concentrations of PST elicited certain effects on shortening PT when compared with NC, and PT value of PST at the initial concentration of 0.31 mg/mL was 4.47 ± 0.45 s, lower than that of NC (6.23 ± 0.55 s). Afterwards, PT values of PST were enhanced with the increase of concentration and achieved 15.30 ± 1.14 s at a concentration of 5.00 mg/mL, remarkably ($P < 0.01$) higher than that of NC, and higher ($P > 0.05$) than that of BC. After sulfation, PT-shortening property of PST was gradually switched to the PT-prolonging capacity with the elevation of concentration. When concentration reached 5.00 mg/mL, SPST-2 had begun to exert noticeable ($P < 0.01$) PT-prolonging effect as

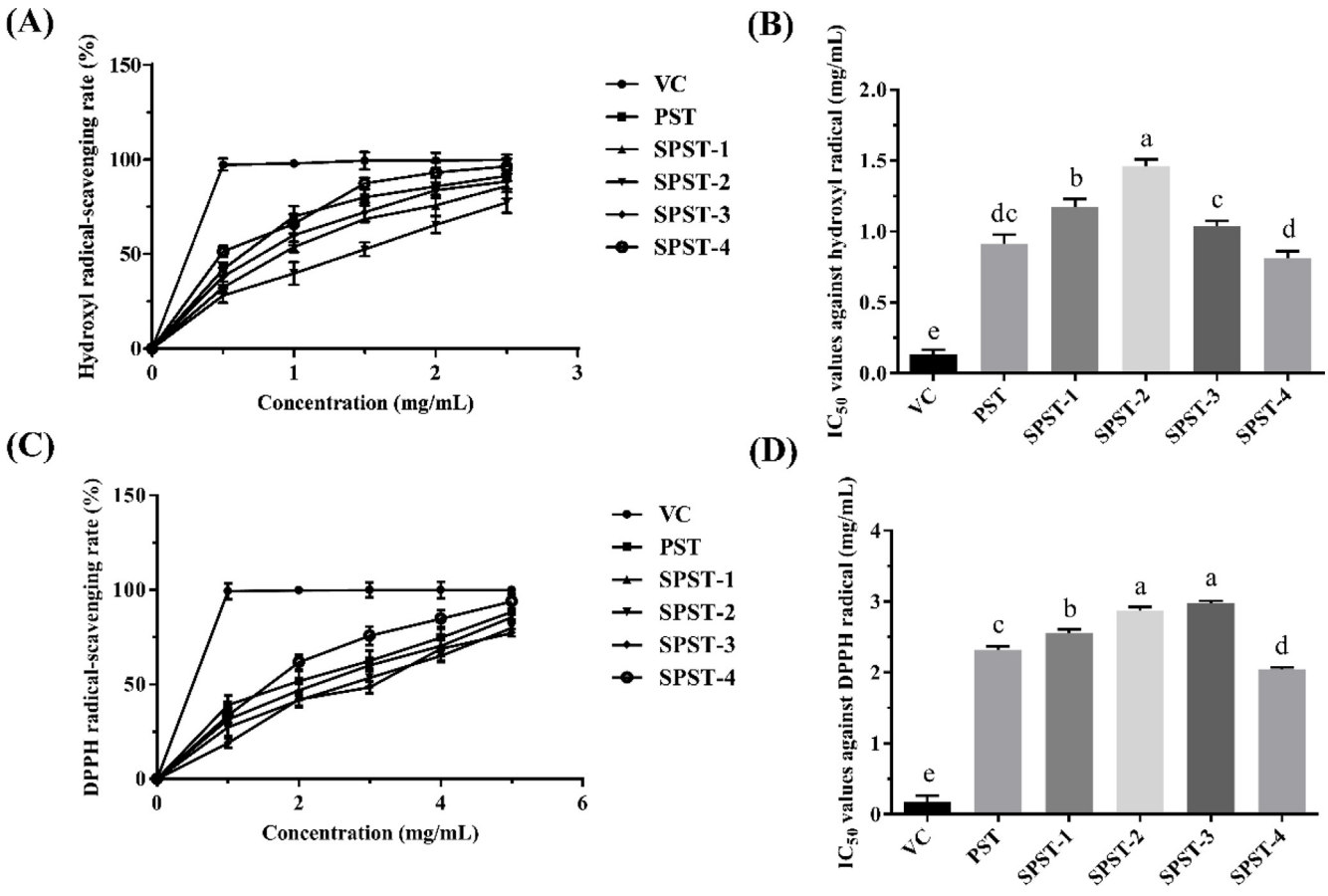

Fig. 6 The antioxidant activities of PST and sulfated derivatives using VC as positive control. (**A**) Profile of hydroxyl radical-scavenging activity; (**B**) Statistical analysis for IC_{50} values against hydroxyl radical; (**C**) Profile of DPPH radical-scavenging activity; (**D**) Statistical analysis for IC_{50} values against DPPH radical. Data were expressed as means ± SD (n = 3). Different letters in lowercase refer to significant differences ($P < 0.05$ or $P < 0.01$).

compared with BC. The results suggested that PST has certain PT-shortening potential, and sulfated modification could convert the innate effect into PT-prolonging activity via extrinsic coagulation pathway (Cao et al., 2019).

Subsequently, the effects of PST and sulfated derivatives on APTT were appraised. As shown in Fig. 7C, APTT values of PST were notably ($P < 0.05$ or $P < 0.01$) smaller than that of BC (31.47 ± 3.41 s) at concentrations ranging from 0.31 to 2.50 mg/mL. The APTT-shortening capacity of PST decreased with the increase of concentration. When concentration was 5.00 mg/mL, APTT value reached 24.27 ± 4.22 s, but still lower ($P > 0.05$) than that of BC. After sulfation, the APTT- prolonging abilities of sulfated derivatives were gradually enhanced in a concentration-dependent manner ($P < 0.05$ or $P < 0.01$). For SPST-1 at 5.00 mg/mL, SPST-2 at concentrations ranging from 1.25 to 5.00 mg/mL, SPST-3 at concentrations ranging from 0.63 to 5.00 mg/mL, and SPST-4 at concentrations spanning from 1.25 to 5.00 mg/mL, APTT values were all significantly ($P < 0.01$) higher than that of BC, the highest of which was 187.13 ± 9.60 s (SPST-3 at 5.00 mg/mL), slightly larger ($P > 0.05$) than that of PC (182.07 ± 2.77 s). As compared with NC, lower concentrations of PST showed certain effects on shortening APTT, which was inversely proportional to concentration. When the concentration was raised to 5.00 mg/mL, APTT value of PST achieved 24.27 ± 4.22 s, but still smaller than that of BC. Sulfated modification could weaken the APTT-shortening ability of PST. For SPST-3, even at a low concentration of 0.63 mg/mL, APTT value (60.30 ± 1.76 s) was markedly ($P < 0.01$) larger than that of BC. The results implied that PST owns certain APTT-shortening effect, and sulfated modification could change that effect into APTT-prolonging capability via intrinsic coagulation pathway (Wang et al., 2019a, 2019b).

The FIB plays a key role in initiating blood clot formation and its level is inversely proportional to the anticoagulant potential of tested sample (Zhang et al., 2020). Thus, the effects of PST and sulfated derivatives on FIB content were finally estimated. As shown in Fig. 7D, all the tested samples decreased FIB contents in a concentration-dependent manner ($P < 0.05$ or $P < 0.01$). However, even the lowest FIB level of PST (276.46 ± 21.93 mg/dL) was still lower ($P > 0.05$) than that of BC (324.07 ± 28.25 mg/dL), the highest counterpart (1964.67 ± 128.40 mg/dL) was significantly higher ($P < 0.01$) than that of BC and was equivalent to that of NC (2075.57 ± 49.24 mg/dL), suggesting that PST inherently possesses certain FIB- promoting effect, especially for the ones with lower concentrations. In the same way, sulfated modification could attenuate the FIB-promoting potential of PST and gradually reverse it into the FIB-lowering activity in a concentration-dependent manner ($P < 0.05$ or $P < 0.01$).

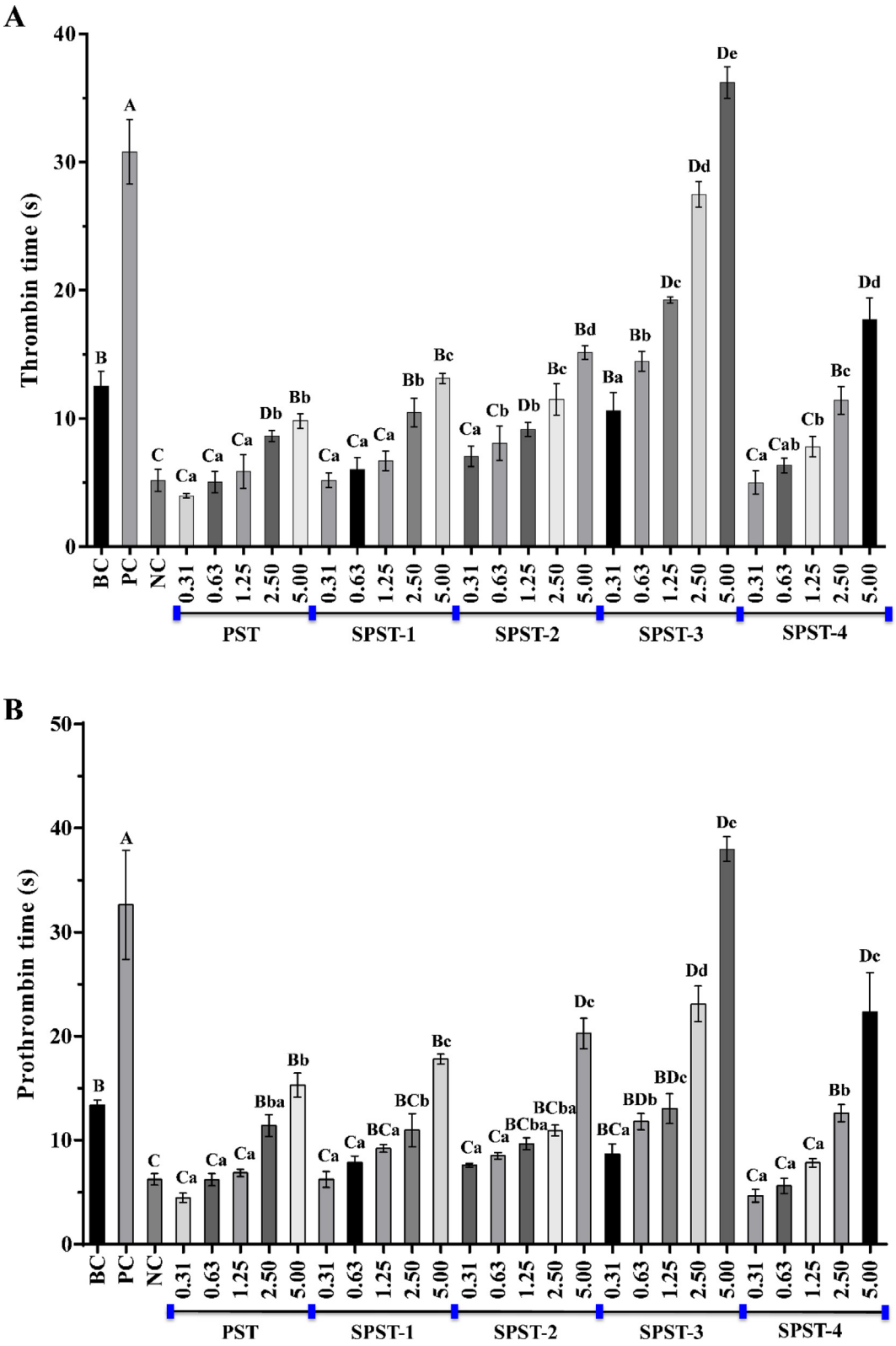

Fig. 7 The effects of PST and sulfated derivatives on thrombin time (**A**), prothrombin time (**B**), activated partial thromboplastin time (**C**) and fibrinogen content (**D**). Data were expressed as means ± SD in triplicate. Letters in uppercase refer to significant differences ($P < 0.05$ or $P < 0.01$) compared with each control between groups, and letters in lowercase mean significant differences ($P < 0.05$ or $P < 0.01$) within groups.

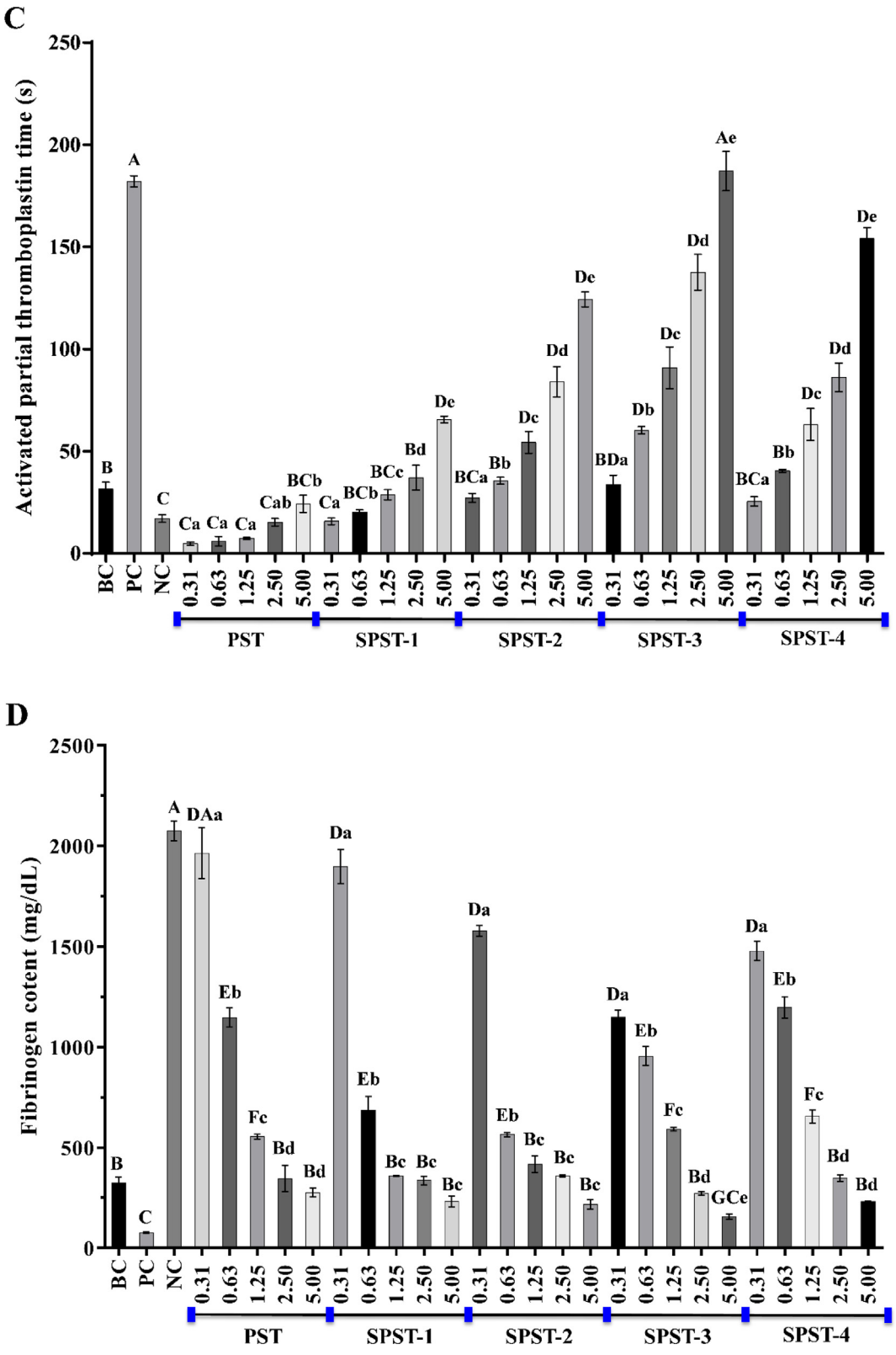

Fig. 7 (*continued*)

Among them, SPST-3 at 5.00 mg/mL elicited the relatively most potency to lower FIB, the FIB level of which was 156.32 ± 13.40 mg/dL, significantly ($P < 0.01$) smaller than that of BC, but still higher ($P > 0.05$) than that of PC, indicating that the sulfated derivatives of PST possess FIB-lowering potentials but are inferior to heparin.

In summary, by combining the above-mentioned results, it could be safely inferred that low-concentration PST has pro-

coagulant potential via activating the intrinsic, extrinsic, and common coagulation pathways as well as by increasing FIB content. This finding was in accordance with the ethnopharmacological uses of *S. trifolia* tuber. The medicinal properties of *S. trifolia* tuber were first recorded in *Mingyi Bielu* in the late Han Dynasty (2nd century BCE), and traditional Chinese medicine holds the opinion that *S. trifolia* tuber can be used for cooling blood to stop bleeding (Zhang et al., 2021a, 2021b). To the best of our knowledge, it would be the first time to conclude that low-concentration PST could be mainly responsible for the hemostatic effect of *S. trifolia* tuber. The pending question is "When to Bleed and When not to Bleed?". Since thousands of years ago, people had attempted to stop bleeding of wounds by applying various topical agents (Achneck et al., 2010). In practical terms, the development of novel hemostatic product is equally important nowadays, owing to the fact that hemorrhage is the leading cause for preventable death in combat trauma and the secondary cause for death in civilian trauma (Peng 2020). With regard to low-concentration PST, it is more likely to provide a promising hit for the discovery of new hemostatic agent. In the following investigation, effects of PST on other indicators relating to hemostatic function, particularly anti-inflammatory ability should be further evaluated. Even though the pro-coagulant capability of PST tended to be weakened with the increase of concentration, any significant differences between PST at the highest concentration and BC were not observed (Fig. 7A ~ 7D). In spite of this, the pro-coagulant or coagulant potentials of high-concentration PST are deserving of deep exploration.

Interestingly, sulfated modification could gradually reverse the innate pro-coagulant potential of PST into anticoagulant effect in a concentration-dependent manner (Fig. 7A ~ 7D). Contrary to PST, sulfated derivatives might exhibit anticoagulant activities via inhibiting the intrinsic, extrinsic, and common coagulation pathways as well as by decreasing FIB content. It is widely recognized that the anticoagulant potential of sulfated polysaccharides relies heavily on the amount of sulfate groups (Chaouch et al., 2018, Rizkyana et al., 2022). Plots for the highest level of anticoagulant biomarkers *vs.* DS supported the contributions of sulfate groups to the anticoagulant activities of sulfated PSTs, in that they give reasonably good linear correlations (R^2 = 0.7625, Fig. 8A; R^2 = 0.7819, Fig. 8B; R^2 = 0.9829, Fig. 8C; R^2 = 0.7582, Fig. 8D). However, when linking the pro-coagulant potential of PST (unmodified but naturally occurring sulfated polysaccharide) to DS, it could be inferred that DS would play a crucial role in the accurate regulation of PST from pro-anticoagulation to anticoagulation, and DS of 0.33 might be the lowest threshold value for PST derivatives to exert anticoagulant effects. These results were consistent with previously published work that slight differences in sulfation of algal galactans account for differences in their anticoagulant and pro-coagulant activities (Fonseca et al., 2008).

The well-acknowledged mechanism of sulfated polysaccharide on anticoagulation is that the negative charges of sulfate groups in sulfated polysaccharide first react with the positive charges of amino acid residues in antithrombin to form a complex that can improve the anticoagulant activity (Groth and Wagenknecht 2001, Fan et al., 2011), and higher DS would be helpful to enhance the interaction. The transient formation

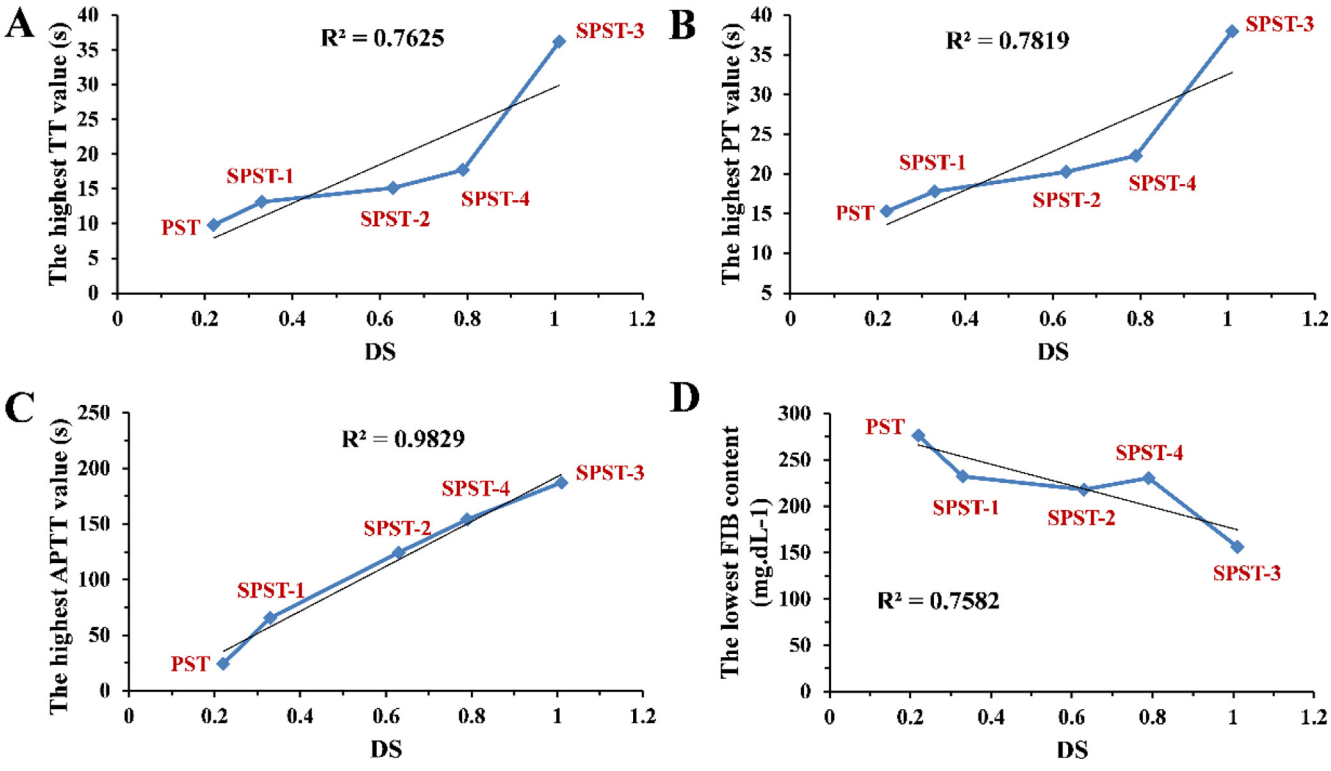

Fig. 8 Relationships between DS and anticoagulant biomarkers for PST and sulfated derivatives showing the linear regression line of best fit. (**A**) DS *vs.* TT; (**B**) DS *vs.* PT; (**C**) DS *vs.* APTT; (**D**) DS *vs.* FIB.

of sulfated polysaccharide-antithrombin complex is then disassociated to form other new complexes, for which the MW of sulfated polysaccharide could be an important factor to regulate the disassociation and combination rates (Wang et al., 2020a, 2020b). From Table 1 and Fig. 7A ~ 7D, it can be noted that SPST-3 with MW of 255.7 kDa exerted better anticoagulant potentials than those of the counterparts with the highest MW (PST) and the lowest MW (SPST-4), respectively, suggesting that proper molecular scale, not too small or too large could be equally important for the implementation of anticoagulant activity of sulfated polysaccharide. The concrete modulatory mechanisms are pending to be explored.

In general, the structures-antioxidant and anticoagulant activities relationships of sulfated polysaccharides are not yet fully elaborated. In addition to DS and MW, other structural parameters, such as repeating units, glycosidic linkages, saccharide sequences, and conformational characteristics would be certain to affect the anticoagulant potential of sulfated polysaccharide, those of which deserve more attention. As for sulfated derivatives of PST, especially SPST-3, a promising anticoagulant candidate, and SPST-4, a potential antioxidant, fully and deeply structural elucidations will be centered in our research.

4. Conclusion

The sulfated modification opens a door to enhance the bioactivities of natural polysaccharides. PST is a naturally occurring sulfated polysaccharide with DS of 0.22. After sulfation, the antioxidant capacity of PST was first lowered, then elevated with the increase of DS. The sulfated derivative SPST-4 with moderate DS and smallest MW showed higher scavenging capacities against hydroxyl and DPPH radicals, particularly for DPPH radical. Although PST is a naturally occurring sulfated polysaccharide, but, interestingly, it exhibited pro-coagulant potential, especially at a low concentration of 0.31 mg/mL, which was even equivalent to that of YNBY (a famous traditional Chinese hemostatic drug). After sulfation, the pro-coagulant potential of PST was gradually switched to anticoagulant activity with the increase of DS, of which SPST-3, the sulfated derivative with highest DS of 1.01 possessed promising anticoagulant potential. At a concentration of 5.00 mg/mL, the effects of SPST-3 on TT and PT outperformed those of heparin at the same concentration. Therefore, DS plays a vital role in regulating the pro-coagulant and anticoagulant properties of PST, even minor differences accounted for the reversion of bioactivity from pro-coagulation to anticoagulation. In a word, PST at lower concentration would be considered as potential hemostatic candidate, and the sulfated derivatives SPST-3 and SPST-4 could possess potentials to be developed as novel antioxidant and anticoagulant agents.

Declaration of Competing Interest

The authors declare that they have no known competing financial interests or personal relationships that could have appeared to influence the work reported in this paper.

Acknowledgement

This work was supported by the Suzhou Science and Technology Bureau (Grant Nos. SNG2022060 and SKY2022127), the Changshu Science and Technology Bureau (Grant Nos. CS202118 and CS202131), the Changshu Health Committee (Grant No. csws202004), and the Nanjing University of Chinese Medicine (Grant No. XZR2020064).

Appendix A. Supplementary material

Supplementary data to this article can be found online at https://doi.org/10.1016/j.arabjc.2023.104812.

References

Accurso, V., Santoro, M., Mancuso, S., et al, 2020. Cardiovascular risk in essential thrombocythemia and polycythemia vera: thrombotic risk and survival. Mediterr. J. Hematol. Infect. Dis. 12, e2020008.

Achneck, H.E., Sileshi, B., Jamiolkowski, R.M., et al, 2010. A comprehensive review of topical hemostatic agents: efficacy and recommendations for use. Ann. Surg. 251, 217–228. https://doi.org/10.1097/SLA.0b013e3181c3bcca.

Adrien, A., Dufour, D., Baudouin, S., et al, 2017. Evaluation of the anticoagulant potential of polysaccharide-rich fractions extracted from macroalgae. Nat. Prod. Res. 31, 2126–2136. https://doi.org/10.1080/14786419.2017.1278595.

Amini, M., Zayeri, F., Salehi, M., 2021. Trend analysis of cardiovascular disease mortality, incidence, and mortality-to-incidence ratio: results from global burden of disease study 2017. BMC Public Health. 21, 401. https://doi.org/10.1186/s12889-021-10429-0.

Arata, P.X., Genoud, V., Lauricella, A.M., et al, 2017. Alterations of fibrin networks mediated by sulfated polysaccharides from green seaweeds. Thromb. Res. 159, 1–4. https://doi.org/10.1016/j.thromres.2017.09.014.

Bai, Y., Qian, J., 2015. Preparation of sulfated barley polysaccharide with sulfamic acid. Food Sci. Technol. 40, 203–208. https://doi.org/10.13684/j.cnki.spkj.2015.03.050.

Cai, Y., Chen, P., Wu, C., et al, 2018b. Sulfated modification and biological activities of polysaccharides derived from Zizyphus jujuba cv. Jinchangzao. Int. J. Biol. Macromol. 120, 1149–1155. https://doi.org/10.1016/j.ijbiomac.2018.08.141.

Cai, Z.X., Wei, Y., Guo, Y.L., et al, 2020. Influence of the degree of esterification of soluble soybean polysaccharide on the stability of acidified milk drinks. Food Hydrocolloid. 108,. https://doi.org/10.1016/j.foodhyd.2020.106052 106052.

Cai, W.R., Xie, L.L., Chen, Y., et al, 2013. Purification, characterization and anticoagulant activity of the polysaccharides from green tea. Carbohydr. Polym. 92, 1086–1090. https://doi.org/10.1016/j.carbpol.2012.10.057.

Cai, L., Zou, S., Liang, D., et al, 2018a. Structural characterization, antioxidant and hepatoprotective activities of polysaccharides from Sophorae tonkinensis Radix. Carbohydr. Polym. 184, 354–365. https://doi.org/10.1016/j.carbpol.2017.12.083.

Cao, S., He, X., Qin, L., et al, 2019. Anticoagulant and antithrombotic properties in vitro and in vivo of a novel sulfated polysaccharide from marine green alga Monostroma nitidum. Mar. Drugs. 17, 247. https://doi.org/10.3390/md17040247.

Caputo, H.E., Straub, J.E., Grinstaff, M.W., 2019. Design, synthesis, and biomedical applications of synthetic sulphated polysaccharides. Chem. Soc. Rev. 48, 2338–2365. https://doi.org/10.1039/c7cs00593h.

Chang, S.C., Hsu, B.Y., Chen, B.H., 2010. Structural characterization of polysaccharides from Zizyphus jujuba and evaluation of antioxidant activity. Int. J. Biol. Macromol. 47, 445–453. https://doi.org/10.1016/j.ijbiomac.2010.06.010.

Chaouch, M.A., Hammi, K.M., Dhahri, M., et al, 2018. Access to new anticoagulant by sulfation of pectin-like polysaccharides isolated from Opuntia ficus indica cladodes. Int. J. Biol. Macromol. 120, 1794–1800. https://doi.org/10.1016/j.ijbiomac.2018.09.130.

Chen, X., Li, X., Xu, X., et al, 2021. Ferroptosis and cardiovascular disease: Role of free radical-induced lipid peroxidation. Free Radic. Res. 55, 405–415. https://doi.org/10.1080/10715762.2021.1876856.

Chen, R., Liu, Z., Zhao, J., et al, 2011. Antioxidant and immunobiological activity of water-soluble polysaccharide fractions purified from Acanthopanax senticosu. Food Chem. 127, 434–440. https://doi.org/10.1016/j.foodchem.2010.12.143.

Chen, Y., Ou, X., Yang, J., et al, 2020. Structural characterization and biological activities of a novel polysaccharide containing N-acetylglucosamine from Ganoderma sinense. Int. J. Biol. Macromol. 158, 1204–1215. https://doi.org/10.1016/j.ijbiomac.2020.05.028.

Chen, T.L., Zhang, M., Li, J.L., et al, 2016. Structural characterization and hypoglycemic activity of Trichosanthes peel polysaccharide. LWT-Food Sci. Technol. 70, 55–62. https://doi.org/10.1016/j.lwt.2016.02.024.

Chen, J., Zhang, X., Huo, D., et al, 2019. Preliminary characterization, antioxidant and alpha-glucosidase inhibitory activities of polysaccharides from Mallotus furetianus. Carbohydr. Polym. 215, 307–315. https://doi.org/10.1016/j.carbpol.2019.03.099.

Cheong, K.L., Yu, B., Chen, J., et al, 2022. A comprehensive review of the cardioprotective effect of marine algae polysaccharide on the gut microbiota. Foods. 11, 3550. https://doi.org/10.3390/foods11223550.

Ciancia, M., Quintana, I., Cerezo, A.S., 2010. Overview of anticoagulant activity of sulfated polysaccharides from seaweeds in relation to their structures, focusing on those of green seaweeds. Curr. Med. Chem. 17, 2503–2529. https://doi.org/10.2174/092986710791556069.

Deng, X., Ke, X., Tang, Y., et al, 2020. Sagittaria sagittifolia polysaccharide interferes with arachidonic acid metabolism in non-alcoholic fatty liver disease mice via Nrf2/HO-1 signaling pathway. Biomed. Pharmacother. 132,. https://doi.org/10.1016/j.biopha.2020.110806 110806.

Du, Z., Shi, F., Liu, D., et al, 2016. Anticoagulant activity of a sulfated Lachnum polysaccharide in mice with a state of hypercoagulability. Bioorg. Med. Chem. Lett. 26, 5550–5556. https://doi.org/10.1016/j.bmcl.2016.09.079.

Dubois, M., Gilles, K.A., Hamilton, J.K., et al, 1956. Colorimetric method for determination of sugars and related substances. Anal. Chem. 28, 350–356. https://doi.org/10.1021/ac60111a017.

Essayem, N., Martin, V., Riondel, A., et al, 2007. Esterification of acrylic acid with but-1-ene over sulfated Fe- and Mn-promoted zirconia. Appl. Catal. A: Gen. 326, 74–81. https://doi.org/10.1016/j.apcata.2007.03.038.

Evans, M.A., Sano, S., Walsh, K., 2020. Cardiovascular disease, aging, and clonal hematopoiesis. Annu. Rev. Pathol. 15, 419–438. https://doi.org/10.1146/annurev-pathmechdis-012419-032544.

Fan, L., Jiang, L., Xu, Y., et al, 2011. Synthesis and anticoagulant activity of sodium alginate sulfates. Carbohydr. Polym. 83, 1797–1803. https://doi.org/10.1016/j.carbpol.2010.10.038.

Fonseca, R.J., Oliveira, S.N., Melo, F.R., et al, 2008. Slight differences in sulfation of algal galactans account for differences in their anticoagulant and venous antithrombotic activities. Thromb. Haemost. 99, 539–545. https://doi.org/10.1160/TH07-10-0603.

Gao, Y.F., Zhou, Y.B., Zhang, Q., et al, 2017. Hydrothermal extraction, structural characterization, and inhibition HeLa cells proliferation of functional polysaccharides from Chinese tea Zhongcha 108. J. Funct. Foods. 39, 1–8. https://doi.org/10.1016/j.jff.2017.09.057.

Groth, T., Wagenknecht, W., 2001. Anticoagulant potential of regioselective derivatized cellulose. Biomaterials. 22, 2719–2729. https://doi.org/10.1016/S0142-9612(01)00013-8.

Gu, J., Zhang, H., Wen, C., et al, 2020a. Purification, characterization, antioxidant and immunological activity of polysaccharide from Sagittaria sagittifolia L. Food Res. Int. 136,. https://doi.org/10.1016/j.foodres.2020.109345 109345.

Gu, J., Zhang, H., Yao, H., et al, 2020b. Comparison of characterization, antioxidant and immunological activities of three polysaccharides from Sagittaria sagittifolia L. Carbohydr. Polym. 235,. https://doi.org/10.1016/j.carbpol.2020.115939 115939.

Gu, J., Zhang, H., Zhang, J., et al, 2020c. Preparation, characterization and bioactivity of polysaccharide fractions from Sagittaria sagittifolia L. Carbohydr. Polym. 229,. https://doi.org/10.1016/j.carbpol.2019.115355 115355.

Gu, J., Zhang, H., Zhang, J., et al, 2020d. Optimization, characterization, rheological study and immune activities of polysaccharide from Sagittaria sagittifolia L. Carbohydr. Polym. 246,. https://doi.org/10.1016/j.carbpol.2020.116595 116595.

Guo, H., Zhang, J., Wang, X., et al, 2010. Sulfated modification, characterization and structure-antioxidant relationships of Artemisia sphaerocephala polysaccharides. Carbohydr. Polym. 81, 897–905. https://doi.org/10.1016/j.carbpol.2010.04.002.

Gutierrez, T., Biller, D.V., Shimmield, T., et al, 2012. Metal binding properties of the EPS produced by Halomonas sp. TG39 and its potential in enhancing trace element bioavailability to eukaryotic phytoplankton. Biometals. 25, 1185–1194. https://doi.org/10.1007/s10534-012-9581-3.

Helfer, H., Siguret, V., Mahe, I., 2020. Tinzaparin sodium pharmacokinetics in patients with chronic kidney disease: Practical implications. Am. J. Cardiovasc. Drugs. 20, 223–228. https://doi.org/10.1007/s40256-019-00382-0.

Hou, N., Zhang, M., Xu, Y., et al, 2017. Polysaccharides and their depolymerized fragments from Costaria costata: Molecular weight and sulfation-dependent anticoagulant and FGF/FGFR signal activating activities. Int. J. Biol. Macromol. 105, 1511–1518. https://doi.org/10.1016/j.ijbiomac.2017.06.042.

Hou, J.T., Zhang, M., Liu, Y., et al, 2020. Fluorescent detectors for hydroxyl radical and their applications in bioimaging: A review. Coordin. Chem. Rev. 421,. https://doi.org/10.1016/j.ccr.2020.213457 213457.

Hu, Z., Wang, P., Zhou, H., et al, 2018. Extraction, characterization and in vitro antioxidant activity of polysaccharides from Carex meyeriana Kunth using different methods. Int. J. Biol. Macromol. 120, 2155–2164. https://doi.org/10.1016/j.ijbiomac.2018.09.125.

Hu, Z., Zhou, H., Li, Y., et al, 2019. Optimized purification process of polysaccharides from Carex meyeriana Kunth by macroporous resin, its characterization and immunomodulatory activity. Int. J. Biol. Macromol. 132, 76–86. https://doi.org/10.1016/j.ijbiomac.2019.03.207.

Huang, L., Huang, M., Shen, M., et al, 2019a. Sulfated modification enhanced the antioxidant activity of Mesona chinensis Benth polysaccharide and its protective effect on cellular oxidative stress. Int. J. Biol. Macromol. 136, 1000–1006. https://doi.org/10.1016/j.ijbiomac.2019.06.199.

Huang, L.X., Shen, M.Y., Morris, G.A., et al, 2019b. Sulfated polysaccharides: Immunomodulation and signaling mechanisms. Trends Food Sci. Tech. 92, 1–11. https://doi.org/10.1016/j.tifs.2019.08.008.

Ji, X.L., Peng, Q., Yuan, Y.P., et al, 2017. Isolation, structures and bioactivities of the polysaccharides from jujube fruit (Ziziphus jujuba Mill.): A review. Food Chem. 227, 349–357. https://doi.org/10.1016/j.foodchem.2017.01.074.

Jia, Y., Xue, Z., Wang, Y., et al, 2021. Chemical structure and inhibition on alpha-glucosidase of polysaccharides from corn silk by fractional precipitation. Carbohydr Polym. 252,. https://doi.org/10.1016/j.carbpol.2020.117185 117185.

Kang, J., Jia, X., Wang, N.F., et al, 2022. Insights into the structure-bioactivity relationships of marine sulfated polysaccharides: A review. Food Hydrocolloid. 123,. https://doi.org/10.1016/j.foodhyd.2021.107049 107049.

Kazachenko, A.S., Malyar, Y.N., Vasilyeva, N.Y., et al, 2021. Optimization of guar gum galactomannan sulfation process with sulfamic acid. Biomass Conv. Bioref. https://doi.org/10.1007/s13399-021-01895-y.

Ke, X.H., Wang, C.G., Luo, W.Z., et al, 2018. Metabolomic study to determine the mechanism underlying the effects of Sagittaria

sagittifolia polysaccharide on isoniazid- and rifampicin-induced hepatotoxicity in mice. Molecules. 23, 3087. https://doi.org/10.3390/molecules23123087.

Khalid, W., Badshah, A., Khan, A.U., et al, 2018. Synthesis, characterization, molecular docking evaluation, antiplatelet and anticoagulant actions of 1,2,4 triazole hydrazone and sulphonamide novel derivatives. Chem. Cent. J. 12, 11. https://doi.org/10.1186/s13065-018-0378-5.

Li, Y., Hu, Z., Wang, X., et al, 2020. Characterization of a polysaccharide with antioxidant and anti-cervical cancer potentials from the corn silk cultivated in Jilin province. Int. J. Biol. Macromol. 155, 1105–1113. https://doi.org/10.1016/j.ijbiomac.2019.11.077.

Liang, L., Ao, L., Ma, T., et al, 2018. Sulfated modification and anticoagulant activity of pumpkin (Cucurbita pepo, Lady Godiva) polysaccharide. Int. J. Biol. Macromol. 106, 447–455. https://doi.org/10.1016/j.ijbiomac.2017.08.035.

Lippi, G., Franchini, M., Targher, G., 2011. Arterial thrombus formation in cardiovascular disease. Nat. Rev. Cardiol. 8, 502–512. https://doi.org/10.1038/nrcardio.2011.91.

Liu, Y., Liu, C., Tan, H., et al, 2009. Sulfation of a polysaccharide obtained from Phellinus ribis and potential biological activities of the sulfated derivatives. Carbohydr. Polym. 77, 370–375. https://doi.org/10.1016/j.carbpol.2009.01.008.

Liu, X., Ren, Z., Yu, R., et al, 2021. Structural characterization of enzymatic modification of Hericium erinaceus polysaccharide and its immune-enhancement activity. Int. J. Biol. Macromol. 166, 1396–1408. https://doi.org/10.1016/j.ijbiomac.2020.11.019.

Liu, Y., Tang, Q., Duan, X., et al, 2018. Antioxidant and anticoagulant activities of mycelia polysaccharides from Catathelasma ventricosum after sulfated modification. Ind. Crop. Prod. 112, 53–60. https://doi.org/10.1016/j.indcrop.2017.10.064.

Lu, X., Mo, X., Guo, H., et al, 2012. Sulfation modification and anticoagulant activity of the polysaccharides obtained from persimmon (Diospyros kaki L.) fruits. Int. J. Biol. Macromol. 51, 1189–1195. https://doi.org/10.1016/j.ijbiomac.2012.08.028.

Mensah, G.A., Roth, G.A., Fuster, V., 2019. The global burden of cardiovascular diseases and risk factors: 2020 and beyond. J. Am. Coll. Cardiol. 74, 2529–2532. https://doi.org/10.1016/j.jacc.2019.10.009.

Mulloy, B., 2005. The specificity of interactions between proteins and sulfated polysaccharides. An. Acad. Bras. Cienc. 77, 651–664. https://doi.org/10.1590/s0001-37652005000400007.

Na, W., Lin, M., Xie, X., et al, 2015. The effect of extraction and purification process on anticoagulant activity of polysaccharide of jujube. J. Chin. Inst. Food Sci. Technol. 15, 141–146. https://doi.org/10.16429/j.1009-7848.2015.10.019.

Nie, C., Zhu, P., Ma, S., et al, 2018. Purification, characterization and immunomodulatory activity of polysaccharides from stem lettuce. Carbohydr. Polym. 188, 236–242. https://doi.org/10.1016/j.carbpol.2018.02.009.

Pan, X., Liu, F., 2006. Research progress on Sagittaria trifolia. Northwest Pharm. J. 21, F0004. https://doi.org/10.3969/j.issn.1004-2407.2006.03.035.

Panda, P., Verma, H.K., Lakkakula, S., et al, 2022. Biomarkers of oxidative stress tethered to cardiovascular diseases. Oxid. Med. Cell. Longev. 2022, 9154295. https://doi.org/10.1155/2022/9154295.

Peng, H.T., 2020. Hemostatic agents for prehospital hemorrhage control: A narrative review. Military Med. Res. 7, 444–463. https://doi.org/10.1186/s40779-020-00241-z.

Qian, J., Bai, Y., Tang, J., et al, 2015. Antioxidation and α-glucosidase inhibitory activities of barley polysaccharides modified with sulfation. LWT-Food Sci. Technol. 64, 104–111. https://doi.org/10.1016/j.lwt.2015.05.034.

Rizkyana, A.D., Ho, T.C., Roy, V.C., et al, 2022. Sulfation and characterization of polysaccharides from Oyster mushroom (Pleurotus ostreatus) extracted using subcritical water. J. Supercrit. Fluid. 179,. https://doi.org/10.1016/j.supflu.2021.105412 105412.

Roman, Y., Barddal, H.P.D., Iacomini, M., et al, 2017. Anticoagulant and antithrombotic effects of chemically sulfated fucogalactan and citrus pectin. Carbohydr. Polym. 174, 731–739. https://doi.org/10.1016/j.carbpol.2017.06.110.

Shalaby, A., Ragab, T., Mehany, A., et al, 2018. Antitumor and prebiotic activities of novel sulfated acidic polysaccharide from ginseng. Biocatal. Agric. Biotechnol. 14, 402–409. https://doi.org/10.1016/j.bcab.2018.04.008.

Song, J., Wu, Y., Jiang, G., et al, 2019. Sulfated polysaccharides from Rhodiola sachalinensis reduce d-gal-induced oxidative stress in NIH 3T3 cells. Int. J. Biol. Macromol. 140, 288–293. https://doi.org/10.1016/j.ijbiomac.2019.08.052.

Stanger, M.J., Thompson, L.A., Young, A.J., et al, 2012. Anticoagulant activity of select dietary supplements. Nutr. Rev. 70, 107–117. https://doi.org/10.1111/j.1753-4887.2011.00444.x.

Tan, R., Wang, H., 2016. Talking about Sagittaria trifolia as medicine and food. J. Clin. Med. Lit. 3, 6700–6701. https://doi.org/10.16281/j.cnki.jocml.2016.33.136.

Tang, Z.L., Wang, X., Yi, B., et al, 2009. Effects of the preoperative administration of Yunnan Baiyao capsules on intraoperative blood loss in bimaxillary orthognathic surgery: a prospective, randomized, double-blind, placebo-controlled study. Int. J. Oral Maxillofac. Surg. 38, 261–266. https://doi.org/10.1016/j.ijom.2008.12.003.

Uda, M.N.A., Gopinath, S.C.B., Hashim, U., et al, 2021. Production and characterization of graphene from carbonaceous rice straw by cost-effect extraction. 3 Biotech 11, 205. https://doi.org/10.1007/s13205-021-02740-9.

Vilas-Boas, A.A., Pintado, M., Oliveira, A.L.S., 2021. Natural bioactive compounds from food waste: Toxicity and safety concerns. Foods. 10, 1564. https://doi.org/10.3390/foods10071564.

Vo, T.S., Kim, S.K., 2014. Marine-derived polysaccharides for regulation of allergic responses. Adv. Food Nutr. Res. 73, 1–13. https://doi.org/10.1016/B978-0-12-800268-1.00001-9.

Wang, Y., Chen, C., Cao, X., et al, 2015b. Determination of agrochemical residues in aquatic vegetables by solid-phase extraction combined with HPLC spectrometry analyses. Res. Chem. Intermediat. 41, 2841–2853. https://doi.org/10.1007/s11164-013-1393-8.

Wang, C., He, Y., Tang, X., et al, 2020a. Sulfation, structural analysis, and anticoagulant bioactivity of ginger polysaccharides. J. Food Sci. 85, 2427–2434. https://doi.org/10.1111/1750-3841.15338.

Wang, F.L., Ji, Y.B., Yang, B., 2020b. Sulfated modification, characterization and monosaccharide composition analysis of Undaria pinnatifida polysaccharides and anti-tumor activity. Exp. Ther. Med. 20, 630–636. https://doi.org/10.3892/etm.2020.8720.

Wang, L., Li, X., Chen, Z., 2009. Sulfated modification of the polysaccharides obtained from defatted rice bran and their antitumor activities. Int. J. Biol. Macromol. 44, 211–214. https://doi.org/10.1016/j.ijbiomac.2008.12.006.

Wang, H., Li, X., Song, J., 2018a. Vegetable genetic resources in China. Hortic. Plant J. 4, 83–88. https://doi.org/10.1016/j.hpj.2018.03.003.

Wang, L., Liu, H.M., Qin, G.Y., 2017. Structure characterization and antioxidant activity of polysaccharides from Chinese quince seed meal. Food Chem. 234, 314–322. https://doi.org/10.1016/j.foodchem.2017.05.002.

Wang, J., Yang, W., Wang, J., et al, 2015a. Regioselective sulfation of Artemisia sphaerocephala polysaccharide: Characterization of chemical structure. Carbohydr. Polym. 133, 320–327. https://doi.org/10.1016/j.carbpol.2015.07.030.

Wang, J., Luo, W., Li, B., et al, 2018b. Sagittaria sagittifolia polysaccharide protects against isoniazid- and rifampicin-induced hepatic injury via activation of nuclear factor E2-related factor 2 signaling in mice. J. Ethnopharmacol. 227, 237–245. https://doi.org/10.1016/j.jep.2018.09.002.

Wang, Z.J., Xie, J.H., Shen, M.Y., et al, 2018c. Sulfated modification of polysaccharides: Synthesis, characterization and bioactivities. Trends Food Sci. Tech. 74, 147–157. https://doi.org/10.1016/j.tifs.2018.02.010.

Wang, L., Zhang, X., Niu, Y., et al, 2019a. Anticoagulant activity of two novel polysaccharides from flowers of Apocynum venetum L. Int. J. Biol. Macromol. 124, 1230–1237. https://doi.org/10.1016/j.ijbiomac.2018.12.015.

Wang, S.N., Zhao, L.L., Li, Q.H., et al, 2019b. Rheological properties and chain conformation of soy hull water-soluble polysaccharide fractions obtained by gradient alcohol precipitation. Food Hydrocolloid. 91, 34–39. https://doi.org/10.1016/j.foodhyd.2018.12.054.

Wei, Y., Cai, Z.X., Wu, M., et al, 2020. Comparative studies on the stabilization of pea protein dispersions by using various polysaccharides. Food Hydrocolloid. 98,. https://doi.org/10.1016/j.foodhyd.2019.105233 105233.

Xiao, H., Fu, X., Cao, C., et al, 2019. Sulfated modification, characterization, antioxidant and hypoglycemic activities of polysaccharides from Sargassum pallidum. Int. J. Biol. Macromol. 121, 407–414. https://doi.org/10.1016/j.ijbiomac.2018.09.197.

Xie, J.-H., Wang, Z.-J., Shen, M.-Y., et al, 2016. Sulfated modification, characterization and antioxidant activities of polysaccharide from Cyclocarya paliurus. Food Hydrocolloid. 53, 7–15. https://doi.org/10.1016/j.foodhyd.2015.02.018.

Yamamoto, K., Koga, Y., Fujiwara, S., 2001. Binding energies of amorphous CN and SiCN films on X-ray photoelectron spectroscopy. Jpn. J. Appl. Phys. 40, 123. https://doi.org/10.1143/JJAP.40.L123.

Zeng, F.K., Chen, W.B., He, P., et al, 2020. Structural characterization of polysaccharides with potential antioxidant and immunomodulatory activities from Chinese water chestnut peels. Carbohydr. Polym. 246,. https://doi.org/10.1016/j.carbpol.2020.116551 116551.

Zhai, W.C., Wei, E.W., Li, R., et al, 2021. Characterization and evaluation of the pro-coagulant and immunomodulatory activities of polysaccharides from Bletilla striata. ACS Omega. 6, 656–665. https://doi.org/10.1021/acsomega.0c05171.

Zhang, J., Chen, M., Wen, C., et al, 2019a. Structural characterization and immunostimulatory activity of a novel polysaccharide isolated with subcritical water from Sagittaria sagittifolia L. Int. J. Biol. Macromol. 133, 11–20. https://doi.org/10.1016/j.ijbiomac.2019.04.077.

Zhang, Y., Liu, Y., Zhu, K., et al, 2018. Acute toxicity, antioxidant, and antifatigue activities of protein-rich extract from Oviductus ranae. Oxid. Med. Cell. Longev. 2018, 9021371. https://doi.org/10.1155/2018/9021371.

Zhang, Y., Wang, G.C., Kong, Y.Q., et al, 2020. A comparative analysis of the essential oils from two species of garlic seedlings cultivated in China: Chemical profile and anticoagulant potential. Food Funct. 11, 6020–6027. https://doi.org/10.1039/D0FO00845A.

Zhang, J., Wen, C., Chen, M., et al, 2019b. Antioxidant activities of Sagittaria sagittifolia L. polysaccharides with subcritical water extraction. Int. J. Biol. Macromol. 134, 172–179. https://doi.org/10.1016/j.ijbiomac.2019.05.047.

Zhang, Y., Zhang, J., Mo, X., et al, 2010. Modification, characterization and structure-anticoagulant activity relationships of persimmon polysaccharides. Carbohydr. Polym. 82, 515–520. https://doi.org/10.1016/j.carbpol.2010.05.008.

Zhang, Y., Yang, G.H., Wang, X.Y., et al, 2021b. Sagittaria trifolia tuber: bioconstituents, processing, products, and health benefits. J. Sci. Food Agr. 101, 3085–3098. https://doi.org/10.1002/jsfa.10977.

Zhang, H., Zou, P., Zhao, H., et al, 2021a. Isolation, purification, structure and antioxidant activity of polysaccharide from pinecones of Pinus koraiensis. Carbohydr. Polym. 251,. https://doi.org/10.1016/j.carbpol.2020.117078 117078.

Zheng, L., Lin, L., Su, G., et al, 2015. Pitfalls of using 1,1-diphenyl-2-picrylhydrazyl (DPPH) assay to assess the radical scavenging activity of peptides: Its susceptibility to interference and low reactivity towards peptides. Food Res. Int. 76, 359–365. https://doi.org/10.1016/j.foodres.2015.06.045.

Zheng, W., Zhou, L., Lin, L., et al, 2019. Physicochemical characteristics and anticoagulant activities of the polysaccharides from Sea Cucumber Pattalus mollis. Mar. Drugs. 17, 198. https://doi.org/10.3390/md17040198.